Biochemical and Biophysical Research Communications 392 (2010) 460–466

Contents lists available at ScienceDirect

Biochemical and Biophysical Research Communications

journal homepage: www.elsevier.com/locate/ybbrc

# Mitochondrial inhibitors show preferential cytotoxicity to human pancreatic cancer PANC-1 cells under glucose-deprived conditions

Isao Momose [a,*], Shun-ichi Ohba [a], Daisuke Tatsuda [a], Manabu Kawada [a], Tohru Masuda [a], Go Tsujiuchi [b], Takao Yamori [c], Hiroyasu Esumi [d], Daishiro Ikeda [a]

[a] Numazu Bio-Medical Research Institute, Microbial Chemistry Research Center, Shizuoka, Japan
[b] Bioscience Laboratory, Meiji Seika Kaisha, LTD, Kanagawa, Japan
[c] Division of Molecular Pharmacology, Cancer Chemotherapy Center, Japanese Foundation for Cancer Research, Tokyo, Japan
[d] Cancer Physiology Project, Research Center for Innovative Oncology, National Cancer Center Hospital East, Chiba, Japan

ARTICLE INFO

*Article history:*
Received 12 January 2010
Available online 18 January 2010

*Keywords:*
Efrapeptin F
Mitochondria
Glucose
Mitochondrial inhibitors
Nutrient deprivation
Glucose deprivation

ABSTRACT

Large areas of tumor are nutrient-starved and hypoxic due to a disorganized vascular system. Therefore, we screened small molecules to identify cytotoxic agents that function preferentially in nutrient-starved conditions. We found that efrapeptin F had preferential cytotoxicity to nutrient-deprived cells compared with nutrient-sufficient cells. Because efrapeptin F acts as a mitochondrial complex V inhibitor, we examined whether inhibitors of complex I, II, III, and V function as cytotoxic agents preferentially in nutrient-deprived cells. Interestingly, these inhibitors showed preferential cytotoxicity to nutrient-deprived cells and caused cell death under glucose-limiting conditions, irrespective of the presence or absence of amino acids and/or serum. In addition, these inhibitors were preferentially cytotoxic to nutrient-deprived cells even under hypoxic conditions. Further, efrapeptin F showed antitumor activity *in vivo*. These data indicate that mitochondrial inhibitors show preferential cytotoxicity to cancer cells under glucose-limiting conditions, and these inhibitors offer a promising strategy for anticancer therapeutic.



## Introduction

Solid tumors have large areas starved for nutrients and oxygen that arise from immature and irregular distribution of blood vessels [1,2]. In particular, hypovascular tumors such as pancreatic cancers show an inherent ability to tolerate such severe growth conditions. Certain human pancreatic cancer cell lines, including PANC-1, AsPC-1, BxPC-3 and KP-3, exhibit marked environmental tolerance and can survive for prolonged periods of time in nutrient-deprived conditions [3]. Tolerance of these cancer cells to nutrient starvation has been associated with the activity of protein kinase B (PKB)/Akt. The PI3K-AKT-TOR signaling promotes cell proliferation and inhibits apoptosis. In addition, activation of Akt has been reported to stimulate cell survival, transformation, metastasis and angiogenesis [4,5]. Kigamicin D, a novel compound discovered from the culture broth of *Amycolatopsis* sp. ML630-mF1, blocks activation of Akt and exhibits preferential cytotoxicity to cancer cells under nutrient-deprived conditions compared to nutrient-rich conditions [6–8]. AG1024 and I-OMe-AG538, specific inhibitors of insulin-like growth factor-1 receptor tyrosine kinase, are also found to be cytotoxic to nutrient-deprived cells [9]. Therefore, agents active in nutrient-deprived conditions could function as anticancer agents.

Energy production is important for cell survival. The metabolism within a solid tumor is markedly different from that of the surrounding normal tissue [10–13]. Increased aerobic glycolysis is uniquely observed in cancers, thereby cancer cells use elevated amounts of glucose as a carbon source for anabolic reactions. However, part of the tumor is in a state of nutrient depletion. Tumor cells respond to nutrient-deprived conditions and adapt their metabolism to obtain amino acids. Autophagy is a catabolic process by which cells supply amino acids from self-digested organelles; cancer cells are likely to use autophagy to obtain amino acids as alternative energy sources [14]. Thus, their metabolic shift to the tumor microenvironment could represent a possible target for antitumor therapy. In this study, we screened natural products such as microbial metabolites to identify agents that preferentially reduce the survival of nutrient-deprived cancer cells. The screen identified efrapeptin F, which is produced by fungi and functions as a cytotoxic agent preferentially against human pancreatic cancer cells in glucose-limiting conditions.

* Corresponding author. Address: Numazu Bio-Medical Research Institute, Microbial Chemistry Research Center, 18-24 Miyamoto, Numazu, Shizuoka 410-0301, Japan. Fax: +81 55 922 6888.
*E-mail address:* imomose@bikaken.or.jp (I. Momose).

0006-291X/$ - see front matter © 2010 Elsevier Inc. All rights reserved.
doi:10.1016/j.bbrc.2010.01.050

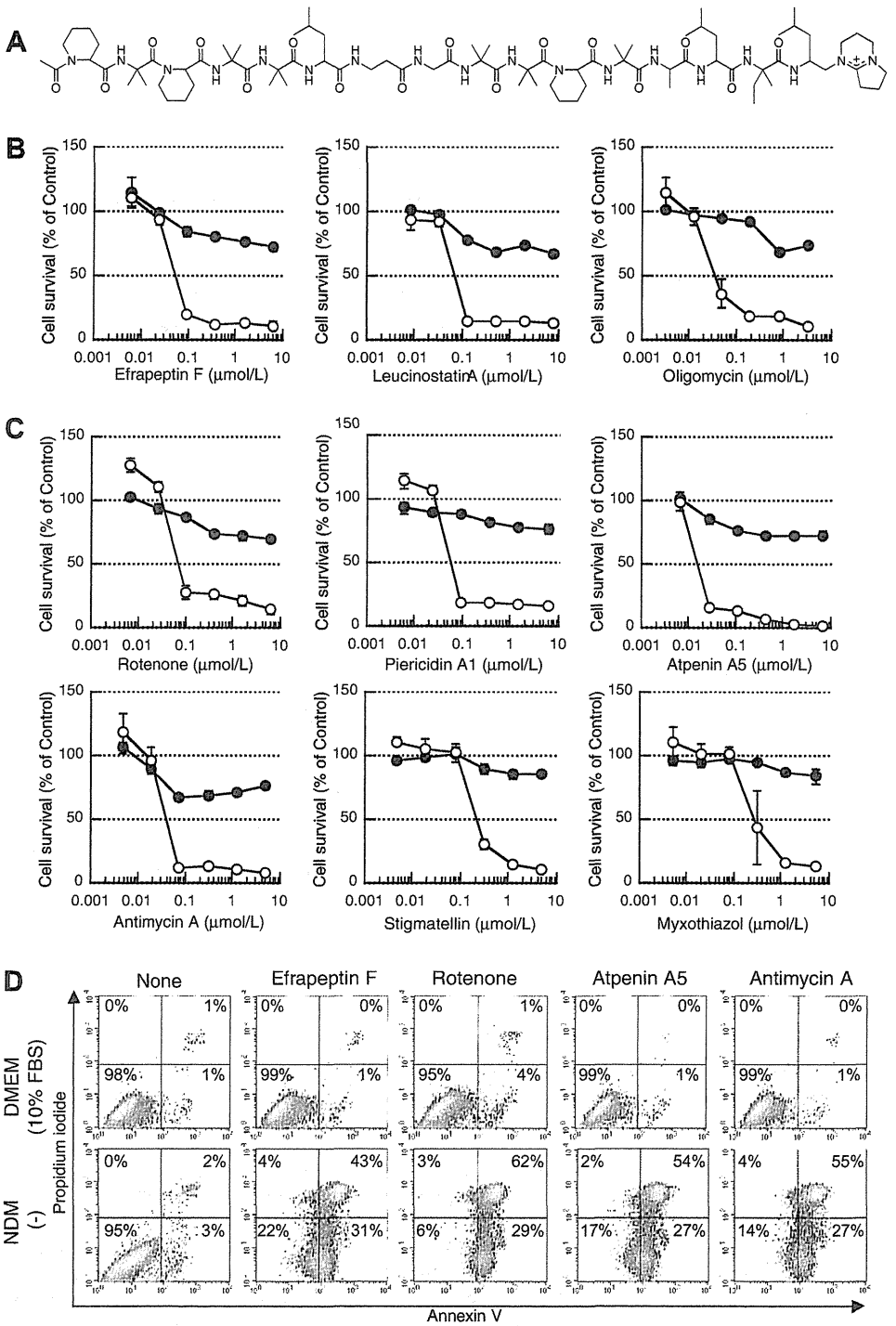


**Fig. 1.** Effect of efrapeptin F and mitochondrial inhibitors on PANC-1 survival under nutrient-deprived conditions. (A) Structure of efrapeptin F. (B) Effect of efrapeptin F and complex V inhibitors (leucinostatin A and oligomycin) on survival of PANC-1 cells in normal medium, DMEM (10% FBS) (●) and nutrient-deprived medium, NDM (−) (○). PANC-1 cells were incubated in DMEM (10% FBS) for 24 h. The cells were then washed with PBS and the medium was replaced with either fresh DMEM (10% FBS) or NDM (−). The indicated concentrations of efrapeptin F and complex V inhibitors were added to each well and the cells were incubated for 24 h. Cell viability was determined using the MTT assay. (C) Effect of complex I, II and III inhibitors on survival of PANC-1 cells in DMEM (10% FBS) (●) and NDM (−) (○). Rotenone and Piericidin $A_1$ were used as complex I inhibitors. Atpenin $A_5$ was as complex II inhibitors. Antimycin A, myxothiazol and stigmatellin were as complex III inhibitors. PANC-1 cells were incubated with inhibitors in DMEM (10% FBS) or NDM (−) for 24 h. (D) Flow cytometric analysis of PANC-1 cells treated with each inhibitor. PANC-1 cells were incubated with 0.1 μmol/L of mitochondrial inhibitors in DMEM (10% FBS) or NDM (−) for 24 h. The cells were stained with annexin V-FITC and propidium iodide and then analyzed using a flow cytometer.

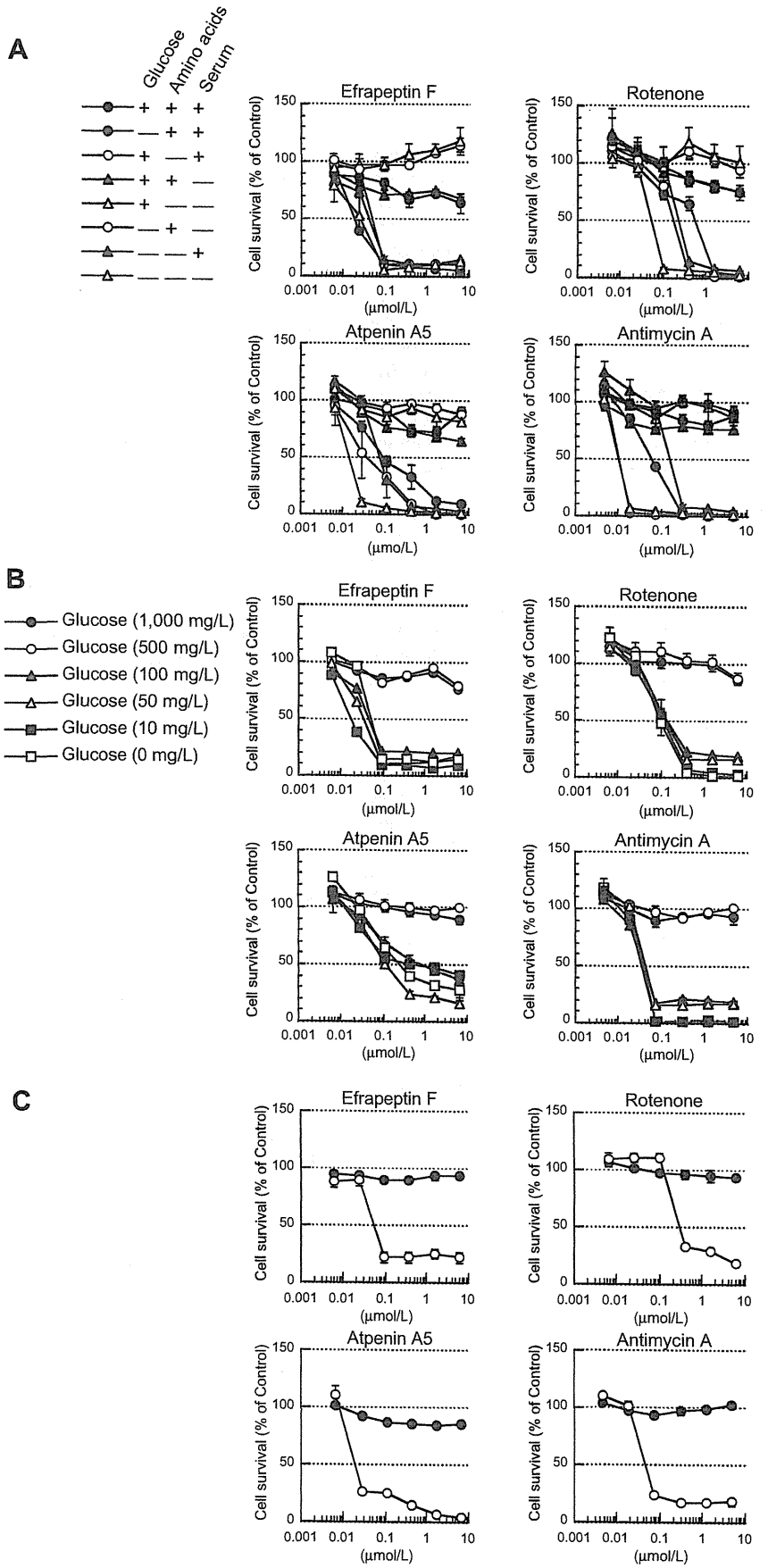
A
Glucose
Amino acids
Serum
Efrapeptin F
Rotenone
Atpenin A5
Antimycin A
Cell survival (% of Control)
(μmol/L)
B
Glucose (1,000 mg/L)
Glucose (500 mg/L)
Glucose (100 mg/L)
Glucose (50 mg/L)
Glucose (10 mg/L)
Glucose (0 mg/L)
C

## Materials and methods

*Inhibitors.* Efrapeptin F and Atpenin $A_5$ were purified from microbial culture extracts supplied by Meiji Seika Kaisha in our laboratory [15–18]. Rotenone and antimycin A were obtained from Sigma–Aldrich (St. Louis, MO).

*Cell lines and culture conditions.* Human pancreatic cancer PANC-1 cells and prostate cancer PC-3 cells were obtained from the American Type Culture Collection (Rockville, MD). Cells were grown at 37 °C with 5% $CO_2$ in Dulbecco's modified Eagle medium (DMEM; Nissui, Tokyo, Japan) supplemented with 10% fetal bovine serum (FBS; Tissue Culture Biologicals, Tulare, CA), 100,000 U/L penicillin G, and 100 mg/L streptomycin. Nutrient starvation was achieved by culturing cells in nutrient-deprived medium (NDM) as previously described [9]. Briefly, the NDM composition was 265 mg/L $CaCl_2{\cdot}H_2O$, 400 mg/L KCl, 200 mg/L $MgSO_4{\cdot}7H_2O$, 6400 mg/L NaCl, 163 mg/L $NaH_2PO_4{\cdot}2H_2O$, 0.1 mg/L $Fe(NO_3)_3{\cdot}9H_2O$, 5 mg/L phenol red, 100,000 U/L penicillin G, 100 mg/L streptomycin, 25 mmol/L HEPES buffer (pH 7.4), and MEM vitamin solution (Invitrogen, Carlsbad, CA); the final pH was adjusted to 7.4 with 10% $NaHCO_3$.

*Preferential cytotoxicity in nutrient-deprived conditions.* PANC-1 cells ($2.5 \times 10^4$ cells/well) in 96-well plates were cultured in DMEM (10% FBS) for 24 h. The cells were washed with PBS and the medium was replaced with either fresh DMEM (10% FBS) or NDM (−). Test samples were added to the well and cells were cultured for 24 h. Furthermore, the medium was replaced with DMEM (10% FBS) containing 0.5 mg/mL thiazolyl blue tetrazolium bromide (MTT; Sigma–Aldrich) and incubated for 3 h to determine cytotoxicity using the MTT assay [19]. Hypoxia was achieved by culturing cells with a mixture of 1% $O_2$, 5% $CO_2$ and 94% $N_2$.

*Measurement of cellular ATP content.* PANC-1 cells ($2.5 \times 10^4$ cells/well) in 96-well plates were cultured in DMEM (10% FBS) for 24 h. The cells were washed with PBS and cultured in fresh DMEM (10% FBS) or NDM (−) with 0.25 μmol/L rotenone, 0.27 μmol/L atpenin $A_5$, 0.10 μmol/L antimycin A or 0.06 μmol/L efrapeptin F for 24 h. The ATP level in cells was determined using the CellTiter-Glo Luminescent Cell Viability Assay (Promega, Madison, WI).

*Flow cytometric analysis.* PANC-1 cells ($5 \times 10^5$) in 60-mm dishes were incubated in DMEM (10% FBS) for 24 h. The cells were washed with PBS and the medium was replaced with either fresh DMEM (10% FBS) or NDM (−). Mitochondrial inhibitors (0.1 μmol/L) were added to the well and the cells were cultured for 24 h. The cells were incubated with annexin V-FITC and propidium iodide according to an annexin V-FITC apoptosis detection kit (Biovision Research Products, Mountain View, CA) and analyzed using a flow cytometer (FACSCalibur; BD Biosciences, Franklin Lakes, NJ).

*Animal experiments.* Male severe combined immunodeficient (SCID) mice, 6 weeks old, were purchased from Charles River Japan (Yokohama, Japan) and maintained in a specific pathogen-free barrier facility according to our institutional guidelines. PC-3 cells ($1 \times 10^7$) were subcutaneously injected into the SCID mouse in the left lateral flank. Five days after inoculation, mice were divided randomly into test groups (control $n = 9$, efrapeptin F-treated $n = 7$) and efrapeptin F was intravenously administered twice weekly for 3 weeks to the efrapeptin F-treated group. Cisplatin was intravenously administered once weekly for 3 weeks. Tumor volume was estimated using the following formula: tumor volume ($mm^3$) = (length × width$^2$)/2.

*Statistical analysis.* All data are representative of three independent experiments with similar results. The statistical data are expressed as mean ± SD using descriptive statistics. Statistical analysis was done by using Student's *t*-test.

## Results

### *Efrapeptin F is preferentially cytotoxic to cancer cells in nutrient-deprived conditions*

To identify cytotoxic agents that function preferentially on nutrient-deprived cancer cells, we screened the cultured media from various microorganisms. One extract of microbial cultured media exhibited preferential cytotoxicity to PANC-1 cells in nutrient-deprived medium (NDM (−)). The extract was subjected to chromatography to obtain a pure compound. The NMR and MS spectra data revealed its chemical structure to be efrapeptin F (Fig. 1A) [15,16]. Efrapeptin F exhibited preferential cytotoxicity to PANC-1 cells in NDM (−), but not in nutrient-sufficient medium (DMEM (10% FBS)) (Fig. 1B). The cytotoxic effect of efrapeptin F on PANC-1 cells in NDM (−) ($IC_{50}$ = 0.052 μmol/L) was more than 100 times stronger than in DMEM (10% FBS) ($IC_{50}$ = >10 μmol/L).

### *Mitochondrial inhibitors are preferentially cytotoxic to cancer cells in nutrient-deprived conditions*

Efrapeptin F has been previously reported to act as an inhibitor of mitochondrial $F_1F_0$-ATPase (complex V) [17]. Therefore, we examined whether mitochondrial complex V inhibitors function as cytotoxic agents preferentially on nutrient-deprived cells (Fig. 1B). Interestingly, leucinostatin A and oligomycin (complex V inhibitors) were more cytotoxic to PANC-1 cells in NDM (−) compared with DMEM (10% FBS) [20,21]. In addition, rotenone and piericidin $A_1$ (NADH-ubiquinone reductase (complex I) inhibitors), atpenin $A_5$ (a succinate-ubiquinone reductase (complex II) inhibitor), antimycin A, stigmatellin and myxothiazol (ubiquinone-cytochrome *c* (complex III) inhibitors) also were more cytotoxic to PANC-1 cells in NDM (−) compare to DMEM (10% FBS) (Fig. 1C) [20–22]. These results clearly demonstrate that mitochondrial inhibitors exhibit preferential cytotoxicity to nutrient-deprived PANC-1 cells. Efrapeptin F (a complex V inhibitor), rotenone (a complex I inhibitor), atpenin $A_5$ (a complex II inhibitor), and antimycin A (a complex III inhibitor) were selected for further study. The mode of cell death caused by mitochondrial inhibitors in nutrient-deprived conditions was examined using annexin V-FITC and propidium iodide double staining and flow cytometry. Mitochondrial inhibitors significantly increased the early-apoptotic and late-apoptotic cells in nutrient-deprived conditions, but not to nutrient-sufficient conditions (Fig. 1D). These results suggested that these inhibitors induce apoptosis in nutrient-deprived cells.

### *Mitochondrial inhibitors are preferentially cytotoxic to cancer cells only under glucose-limiting conditions*

To determine what nutrient component was responsible for cytotoxicity of mitochondrial inhibitors, we examined the effect

**Fig. 2.** Effect of mitochondrial inhibitors on PANC-1 survival under glucose-starved conditions and hypoxic conditions. (A) Effect of nutrient starvation on cytotoxicity of mitochondrial inhibitors. PANC-1 cells were incubated with inhibitors in nutrient-deprived medium containing glucose, amino acids and/or dialyzed FBS for 24 h. (B) Effect of glucose levels on cytotoxicity of mitochondrial inhibitors. PANC-1 cells were incubated with inhibitors in DMEM (10% dialyzed FBS) containing the indicated concentrations of glucose for 24 h. (C) Effect of hypoxia on cytotoxicity of mitochondrial inhibitors. PANC-1 cells were incubated with inhibitors in DMEM (10% FBS) (●) or NDM (−) (○) under 1% $O_2$ for 24 h.

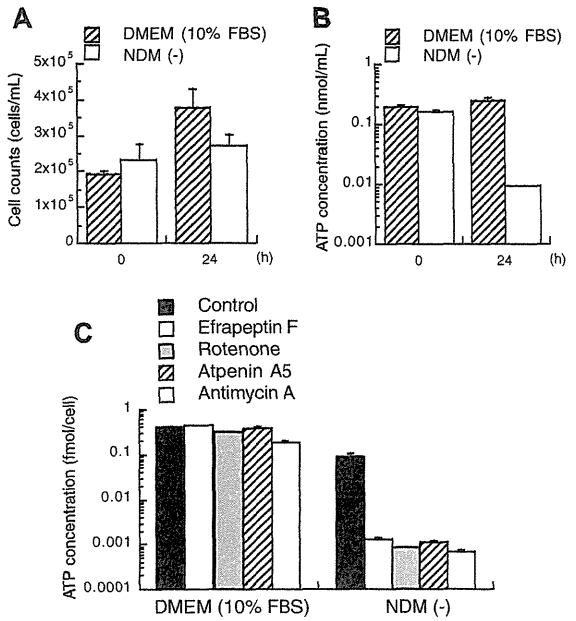


**Fig. 3.** Effect of mitochondrial inhibitors on cellular ATP levels of PANC-1 cells grown in nutrient-deprived medium. (A) Effect of nutrient starvation on PANC-1 cell growth. PANC-1 cells were incubated in DMEM (10% FBS) or NDM (−) for 24 h and cell numbers were measured by cell counting. (B) Cellular ATP levels were determined by the CellTiter-Glo Luminescent Cell Viability Assay after incubation in DMEM (10% FBS) or NDM (−) for 24 h. (C) PANC-1 cells were incubated with 0.25 μmol/L rotenone, 0.27 μmol/L atpenin $A_5$, 0.10 μmol/L antimycin A and 0.06 μmol/L efrapeptin F in DMEM (10% FBS) or NDM (−) for 24 h and cellular ATP levels were determined.

of these inhibitors on PANC-1 cell survival under various nutrient-starved conditions (Fig. 2A). Mitochondrial inhibitors preferentially induced cell death under glucose-deprived conditions, irrespective of the presence or absence of amino acids and/or serum. We then examined the effect of glucose levels on cytotoxicity of these inhibitors (Fig. 2B). The concentration of glucose in DMEM is 1000 mg/L. Mitochondrial inhibitors did not induce cell death in the PANC-1 cells cultured with 1000 and 500 mg/L glucose, but in less than 100 mg/L glucose each inhibitor exhibited cytotoxicity. These results demonstrate clearly that glucose is the key component to determine the sensitivity of cancer cells to mitochondrial inhibitors.

### *Mitochondrial inhibitors are preferentially cytotoxic to nutrient-deprived cells under hypoxic conditions*

Because large areas of tumor are exposed not only to nutrient starvation but also to hypoxic conditions, we examined preferential cytotoxicity of mitochondrial inhibitors to nutrient-deprived cells in hypoxic conditions (Fig. 2C). These inhibitors were more cytotoxic to nutrient-deprived PANC-1 cells in 1% $O_2$ as well as 21% $O_2$. Our results demonstrate that mitochondrial inhibitors show preferentially cytotoxicity to nutrient-deprived cells not only under normoxic conditions but also under hypoxic conditions.

### *Reduction of cellular ATP levels by mitochondrial inhibitors induces preferential cell death to nutrient-deprived cells*

To investigate why mitochondrial inhibitors exhibit preferential cytotoxicity to nutrient-deprived cells, we examined the effect of mitochondrial inhibitors on cellular ATP levels in nutrient-deprived cells. When PANC-1 cells were incubated in NDM (−) for 24 h, the cells grew less and the cellular ATP levels were markedly decreased (Fig. 3A and B). Since PANC-1 cells incubated in NDM (−) for 24 h could hardly be stained by trypan blue, the cells were able to survive in nutrient starvation in spite of lower ATP levels (Fig. S1). When PANC-1 cells were exposed to mitochondrial inhibitors for 24 h, the amount of cellular ATP were slightly decreased in DMEM (10% FBS), whereas in NDM (−) cellular ATP content decreased 100-fold compared to controls (Fig. 3C). These results indicate that depletion of ATP exerts preferential cytotoxicity to nutrient-starved cells.

**Table 1**
Growth inhibitory activity of efrapeptin F against 39 human cancer cell lines in the JFCR39 panel.

| Origin of cancer | Cell line | Log $GI_{50}$ (μmol/L)[a] |
|---|---|---|
| Breast | HBC-4 | −7.22 |
| | BSY-1 | −6.73 |
| | HBC-5 | −8.00 |
| | MCF-7 | −8.00 |
| | MDA-MB-231 | −5.94 |
| Central nervous system | U251 | −7.45 |
| | SF-268 | −6.17 |
| | SF-295 | −8.00 |
| | SF-539 | −6.13 |
| | SNB-75 | −5.79 |
| | SNB-78 | −6.47 |
| Colon | HCC2998 | −6.84 |
| | KM-12 | −6.65 |
| | HT-29 | −6.86 |
| | HCT-15 | −5.61 |
| | HCT-116 | −6.48 |
| Lung | NCI-H23 | −8.00 |
| | NCI-H226 | −6.60 |
| | NCI-H522 | −8.00 |
| | NCI-H460 | −6.69 |
| | A549 | −6.53 |
| | DMS273 | −6.64 |
| | DMS114 | −8.00 |
| Melanoma | LOX-IMVI | −6.71 |
| Ovary | OVCAR-3 | −6.58 |
| | OVCAR-4 | −5.85 |
| | OVCAR-5 | −6.21 |
| | OVCAR-8 | −8.00 |
| | SK-OV-3 | −6.46 |
| Kidney | RXF-631L | −5.17 |
| | ACHN | −5.94 |
| Stomach | St-4 | −6.10 |
| | MKN1 | −6.56 |
| | MKN7 | −8.00 |
| | MKN28 | −8.00 |
| | MKN45 | −6.78 |
| | MKN74 | −8.00 |
| Prostate | DU-145 | −6.76 |
| | PC-3 | −8.00 |
| MG-MID[b] | | −6.87 |
| Delta[c] | | 1.13 |
| Range[d] | | 2.83 |

[a] Log concentration of efrapeptin F for inhibition of cell growth at 50% compared to control.
[b] Mean value of log $GI_{50}$ over all cell lines tested.
[c] The difference in log $GI_{50}$ value of the most sensitive cell and MG-MID value.
[d] The difference in log $GI_{50}$ value of the most sensitive cell and the least sensitive cell.

### *Efrapeptin F inhibits tumor growth in vivo*

PANC-1 cells are low tumorigenicity even in immunodeficient mice. To explore the *in vivo* antitumor activity of mitochondrial inhibitors, we examined the growth inhibitory activity of efrapeptin F against 39 human cancer cell lines of the JFCR39 panel (Table 1) [23–25]. Efrapeptin F exhibited potent growth inhibitory

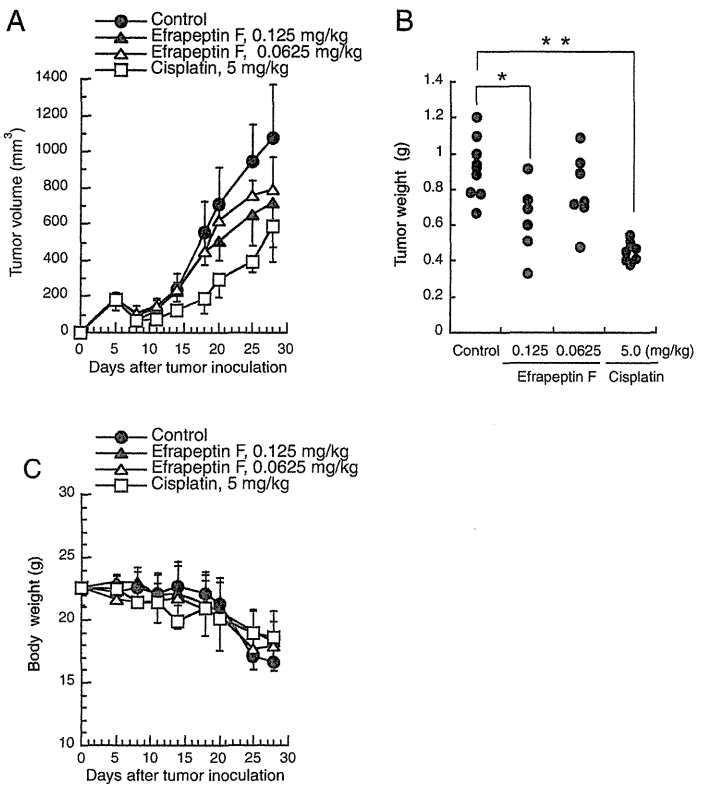


**Fig. 4.** Antitumor effect of efrapeptin F on PC-3 cells in SCID mice. PC-3 cells ($1 \times 10^7$) were subcutaneously inoculated into SCID mice on day 0. Efrapeptin F was administrated intravenously twice weekly for 3 weeks from day 5. (A) Tumor volumes. *Y* axis, tumor volume ($mm^3$); *X* axis, time (day). (B) Tumor weight. The tumors were excised on day 28. $^{**}P < 0.001$; $^{*}P < 0.05$, compared with control (Student's *t*-test). (C) Body weight. *Y* axis, body weight (g); *X* axis, time (day). *Points*, mean values; *bars*, SD.

activity, and the mean value for log concentration for inhibition of cell growth at 50% compared to control was −6.87 (135 μmol/L). In particular, HBC-5, MCF-7, SF-295, NCI-H23, NCI-H522, DMS114, OVCAR-8, MKN7, MKN28, MKN74 and PC-3 cells were sensitive to efrapeptin F. Efrapeptin F showed preferential cytotoxicity to PC-3 cells in nutrient-deprived conditions as well as to PANC-1 cells (Fig. S2). Therefore, xenograft models of PC-3 cells were used to evaluate the *in vivo* antitumor activity of efrapeptin F. Efrapeptin F was intravenously administered twice weekly for 3 weeks from day 5 after the tumor inoculation. Efrapeptin F inhibited tumor growth of the PC-3 xenograft (Fig. 4A and B). Efrapeptin F at 0.125 and 0.0625 mg/kg reduced tumor weight by 68% and 86%, respectively (Tumor weight (g), control = 0.92 ± 0.17 (mean ± SD), 0.125 mg/kg efrapeptin F = 0.63 ± 0.20, 0.0625 mg/kg efrapeptin F = 0.79 ± 0.20) (Fig. 4B). To assess toxicity, we measured the body weight of the tumor-bearing mice (Fig. 4C). Their weight was not reduced by administration of efrapeptin F at these doses. However, among seven mice that were administrated efrapeptin F at a high dose (125 μg/kg), only one mouse died at day 23. Remaining mice survived until the end of the experiment without a decrease of body weight and anatomically without toxic effects in critical organs.

## Discussion

Tumor microenvironment strongly affects tumor development and progression. Many aspects of physiology that differentiate solid tumors from normal tissues arise from differences in vasculature. Disorganized vascular systems in tumors result in large areas of tumor exposed to nutrient starvation and hypoxic conditions. In addition, due to the unregulated growth of tumor cells caused by genetic and epigenetic alterations, tumor cells proliferate more rapidly than normal cells and nutrient and oxygen demands often exceed supply [26–28]. In particular, highly aggressive tumor cells such as pancreatic cancers that are relatively hypovascular, are able to survive even in conditions of low nutrients and low oxygen supply. Since chronic nutrient deprivation seldom occurs in normal tissues, one strategy for anticancer agent development is to target cancer cells growing in nutrient-deprived conditions. Thus, we screened to identify cytotoxic agents that function preferentially in nutrient-deprived cancer cells.

Previous studies have shown that conventional chemotherapeutic drugs and various small molecule inhibitors were only weakly cytotoxic to cancer cells in nutrient-deprived conditions [9]. In this study, we found that the small molecule efrapeptin F, which is produced by some fungi showed preferential cytotoxicity to PANC-1 cells grown in nutrient-deprived conditions compared with cells in nutrient-sufficient conditions. Because efrapeptin F inhibits the mitochondrial complex V, we examined whether mitochondrial complex V inhibitors such as leucinostatin A and oligomycin act as cytotoxic agents preferentially on nutrient-deprived cells. Interestingly, these inhibitors were more cytotoxic to PANC-1 cells in NDM (−) compared to DMEM (10% FBS). In addition, mitochondrial complex I inhibitors (rotenone and piericidin $A_1$), a complex II inhibitor (atpenin $A_5$), and complex III inhibitors (antimycin A, stigmatellin and myxothiazol) also were more cytotoxic to PANC-1 cells in NDM (−). These results clearly demonstrate that mitochondrial inhibitors exhibit preferential cytotoxicity to nutrient-deprived PANC-1 cells, suggesting that mitochondrial inhibitors have unique and attractive characteristics in antitumor agent development. These inhibitors induced cell death under glucose-limiting conditions, irrespective of the presence or absence of amino acids and/or serum. The glucose concentration in colon cancers is only ~1 of 45 of typical plasma glucose concentration (1000 mg/L

or 5.6 nmol/L) [13]. Mitochondrial inhibitors did not induce cell death in 1000 mg/L glucose, but each inhibitors exhibited cytotoxicity in less than 100 mg/L glucose levels. The cytotoxicity caused by mitochondrial inhibitors depended on glucose levels in the culture medium and glucose was the key component to determine the sensitivity of cancer cells to their inhibitors. However, it is unclear how mitochondrial inhibitors exhibit preferential cytotoxicity to nutrient-deprived cells. The cellular ATP level was markedly decreased in PANC-1 cells grown in nutrient starvation. Mitochondrial inhibitors induced ATP depletion in nutrient-deprived cells at lower concentrations of inhibitors compared with nutrient-sufficient cells, thereby these inhibitors could exert preferential cytotoxicity under nutrient-deprived conditions.

Large areas of tumor are exposed not only to nutrient starvation but also hypoxic conditions. Therefore, we examined preferential cytotoxicity of mitochondrial inhibitors to nutrient-deprived cells in hypoxic conditions. Mitochondrial inhibitors showed preferential cytotoxicity to nutrient-deprived cells not only under hypoxic conditions but also under normoxic conditions. Normal tissue uses glycolysis to generate approximately 10% of the cellular ATP, with mitochondria accounting for 90%. In tumor sections, however, over 50% of the cellular ATP is produced by glycolysis with the remainder being generated at the mitochondria [29]. In hypoxic conditions (1% $O_2$), HIF-1α was stabilized and accumulated in nutrient-deprived PANC-1 cells, and the real-time PCR analysis revealed that hexokinase 2 and glucose transporter-1 expression were increased (data not shown). Despite PANC-1 cells grown in nutrient-deprived and hypoxic conditions were represented activation of glycolysis and induction of glucose transporter-1, mitochondrial inhibitors exhibited strong cytotoxicity to these cells. Therefore, ATP generation by mitochondria appeared to be essential for cell survival under hypoxic as well as normoxic conditions.

PANC-1 cells are low tumorigenicity even in SCID mice. To examine the *in vivo* antitumor activity of mitochondrial inhibitors, we explored cancer cell lines that were more sensitive to efrapeptin F. The growth inhibitory activity of efrapeptin F against 39 human cancer cell lines of the JFCR39 panel revealed that human prostate cancer PC-3 cells were highly sensitive to efrapeptin F. Thus, PC-3 cancer xenograft models were used to evaluate *in vivo* antitumor activity, and efrapeptin F was found to induce regression of PC-3 xenograft tumors. In this study, we demonstrated that mitochondrial inhibitors showed preferential cytotoxicity to nutrient-deprived cancer cells relative to nutrient-sufficient cells. Therefore, the potent cytotoxicity of these inhibitors to cancer cells deprived of nutrients (simulating a tumor microenvironment) makes mitochondria a promising target for new drugs that may be developed to treat a broad spectrum of malignant tumors.

## Acknowledgments

This work was supported by a Grant-in-Aid for the Third-Term Comprehensive 10-Years Strategy for Cancer Control from the Ministry of Health, Labour and Welfare in Japan. We thank Ms. S. Kakuda for technical assistance and the Screening Committee of Anticancer Drugs supported by a Grant-in-Aid for Scientific Research on Priority Area "Cancer" from the Ministry of Education, Culture, Sports, Science and Technology, Japan for supplying the measurement of growth inhibitory activities on 39 human cancer cell lines.

## Appendix A. Supplementary data

Supplementary data associated with this article can be found, in the online version, at doi:10.1016/j.bbrc.2010.01.050.

## References

[1] P. Vaupel, F. Kallinowski, P. Okunieff, Blood flow, oxygen and nutrient supply, and metabolic microenvironment of human tumors: a review, Cancer Res. 49 (1989) 6449–6465.
[2] J.M. Brown, A.J. Giaccia, The unique physiology of solid tumors: opportunities (and problems) for cancer therapy, Cancer Res. 58 (1998) 1408–1416.
[3] K. Izuishi, K. Kato, T. Ogura, T. Kinoshita, H. Esumi, Remarkable tolerance of tumor cells to nutrient deprivation: possible new biochemical target for cancer therapy, Cancer Res. 60 (2000) 6201–6207.
[4] R. Baserga, The contradictions of the insulin-like growth factor 1 receptor, Oncogene 19 (2000) 5574–5581.
[5] M.N. Pollak, E.S. Schernhammer, S.E. Hankinson, Insulin-like growth factors and neoplasia, Nat. Rev. Cancer 4 (2004) 505–518.
[6] S. Kunimoto, J. Lu, H. Esumi, Y. Yamazaki, N. Kinoshita, Y. Honma, M. Hamada, M. Ohsono, M. Ishizuka, T. Takeuchi, Kigamicins, novel antitumor antibiotics. I. Taxonomy, isolation, physico-chemical properties and biological activities, J. Antibiot. 56 (2003) 1004–1011.
[7] S. Kunimoto, T. Someno, Y. Yamazaki, J. Lu, H. Esumi, H. Naganawa, Kigamicins, novel antitumor antibiotics. II. Structure determination, J. Antibiot. 56 (2003) 1007–1012.
[8] J. Lu, S. Kunimoto, Y. Yamazaki, M. Kaminishi, H. Esumi, H. Esumi, Kigamicin D, a novel anticancer agent based on a new anti-austerity strategy targeting cancer cells' tolerance to nutrient starvation, Cancer Sci. 95 (2004) 547–552.
[9] I. Momose, S. Kunimoto, M. Osono, D. Ikeda, Inhibitors of insulin-like growth factor-1 receptor tyrosine kinase are preferentially cytotoxic to nutrient-deprived pancreatic cancer cells, Biochem. Biophys. Res. Commun. 380 (2009) 171–176.
[10] N.C. Denko, Hypoxia, HIF1 and glucose metabolism in the solid tumour, Nat. Rev. Cancer 8 (2008) 705–723.
[11] R.A. Gatenby, R.J. Gillies, Why do cancers have high aerobic glycolysis?, Nat Rev. Cancer 4 (2004) 891–899.
[12] G. Kroemer, J. Pouyssegur, Tumor cell metabolism: cancer's Achilles' heel, Cancer Cell 13 (2008) 472–482.
[13] A. Hirayama, K. Kami, M. Sugimoto, M. Sugawara, N. Toki, H. Onozuka, T. Kinoshita, N. Saito, A. Ochiai, M. Tomita, H. Esumi, T. Soga, Quantitative metabolome profiling of colon and stomach cancer microenvironment by capillary electrophoresis time-of-flight mass spectrometry, Cancer Res. 69 (2009) 4918–4925.
[14] B. Levine, D.J. Klionsky, Development by self-digestion: molecular mechanisms and biological functions of autophagy, Dev. Cell 6 (2004) 463–477.
[15] S. Gupta, B.S. Krasnoff, W.D. Roberts, A.A.J. Renwick, S.L. Brinen, J. Clardy, Structures of the efrapeptins: potent inhibitors of mitochondrial ATPase from the fungus *Tolypocladium niveum*, J. Am. Chem. Soc. 113 (1991) 707–709.
[16] S. Gupta, B.S. Krasnoff, W.D. Roberts, A.A.J. Renwick, S.L. Brinen, J. Clardy, Structure of efrapeptins from the fungus *Tolypocladium niveum*: peptide inhibitors of mitochondrial ATPase, J. Org. Chem. 57 (1992) 2306–2313.
[17] R.L. Cross, W.E. Kohlbrenner, The mode of inhibition of oxidative phosphorylation by efrapeptin (A23871). Evidence for an alternating site mechanism for ATP synthesis, J. Biol. Chem. 253 (1978) 4865–4873.
[18] M. Kawada, I. Momose, T. Someno, G. Tsujiuchi, D. Ikeda, New atpenins, NBRI23477A and B, inhibit the growth of human prostate cancer cells, J. Antibiot. 62 (2009) 243–246.
[19] T. Mosmann, Rapid colorimetric assay for cellular growth and survival: application to proliferation and cytotoxicity assays, J. Immunol. Methods 65 (1983) 55–63.
[20] M. Ueki, K. Machida, M. Takeuchi, Antifungal inhibitors of mitochondrial respiration: discovery and prospects for development, Curr. Opin. Investig. Drugs 2 (2000) 387–398.
[21] N. Orme-Johnson, Direct and indirect inhibitors of mitochondrial ATP synthesis, Methods Cell Biol. 80 (2007) 813–826.
[22] H. Miyadera, K. Shiomi, H. Ui, Y. Yamaguchi, R. Masuma, H. Tomoda, H. Miyoshi, A. Osanai, K. Kita, S. Omura, Atpenins, potent and specific inhibitors of mitochondrial complex II (succinate-ubiquinone oxidoreductase), Proc. Natl. Acad. Sci. USA 100 (2003) 473–477.
[23] S. Dan, T. Tsunoda, O. Kitahara, R. Yanagawa, H. Zembutsu, T. Katagiri, K. Yamazaki, Y. Nakamura, T. Yamori, An integrated database of chemosensitivity to 55 anticancer drugs and gene expression profiles of 39 human cancer cell lines, Cancer Res. 62 (2002) 1139–1147.
[24] T. Yamori, Panel of human cancer cell lines provides valuable database for drug discovery and bioinformatics, Cancer Chemother. Pharmacol. 52 (Suppl. 1) (2003) S74–S79.
[25] T. Yamori, A. Matsunaga, S. Sato, K. Yamazaki, A. Komi, K. Ishizu, I. Mita, H. Edatsugi, Y. Matsuba, K. Takezawa, O. Nakanishi, H. Kohno, Y. Nakajima, H. Komatsu, T. Andoh, T. Tsuruo, Potent antitumor activity of MS-247, a novel DNA minor groove binder, evaluated by an in vitro and in vivo human cancer cell line panel, Cancer Res. 59 (1999) 4042–4049.
[26] C.V. Dang, G.L. Semenza, Oncogenic alterations of metabolism, Trends Biochem. Sci. 24 (1999) 68–72.
[27] R.M. Southerland, Cell and environment interactions in tumor microregions: the multicell spheroid model, Science 240 (1988) 178–184.
[28] G. Helmlinger, F. Yuan, M. Dellian, R.K. Jain, Interstitial pH and $pO_2$ gradients in solid tumors in vivo: high-resolution measurements reveal a lack of correlation, Nat. Med. 3 (1997) 177–182.
[29] O. Warburg, On respiratory impairment in cancer cells, Science 124 (1956) 269–270.

JJCO Japanese Journal of Clinical Oncology

*Jpn J Clin Oncol 2010;40(6)537–541*
*doi:10.1093/jjco/hyp197*
Advance Access Publication 4 February 2010

# Usefulness of Narrow-band Imaging for Detecting the Primary Tumor Site in Patients with Primary Unknown Cervical Lymph Node Metastasis

**Tomomasa Hayashi[1,2,3], Manabu Muto[4], Ryuichi Hayashi[3], Keiko Minashi[5], Tomonori Yano[5], Seiji Kishimoto[2] and Satoshi Ebihara[1]**

[1]Department of Head and Neck Surgery, Kyoundo Hospital Sasaki Foundation, [2]Department of Head and Neck Surgery, Tokyo Medical and Dental University Graduate School of Medicine, Tokyo, [3]Department of Head and Neck Surgery, National Cancer Center Hospital East, Chiba, [4]Department of Gastroenterology and Hepatology, Kyoto University Graduate School of Medicine, Kyoto and [5]Department of Gastroenterology, National Cancer Center Hospital East, Chiba, Japan

For reprints and all correspondence: Tomomasa Hayashi, Department of Head and Neck Surgery, Kyoundo Hospital Sasaki Foundation, Tokyo, Japan. E-mail: hayashi@po.kyoundo.jp

Received October 29, 2009; accepted December 24, 2009

**Objective:** We sometimes experienced patients with primary unknown cervical lymph node metastasis. In such cases, if computed tomography, magnetic resonance imaging, laryngoscopy and gastrointestinal endoscopy cannot detect a primary site, there is no other effective method to identify a possible primary tumor. We investigated whether narrow-band imaging can detect a possible primary tumor in such.

**Methods:** Forty-six patients with primary unknown cervical lymph node metastasis were surveyed about primary tumors, from January 2003 to December 2006. All cervical lymph nodes were histologically proved to be squamous cell carcinoma by fine-needle aspiration cytology. Narrow-band imaging combined with magnifying endoscopy was used to identify the primary site in the head and neck region and cervical esophagus. Histological analysis was performed for all suspicious lesions by a biopsy specimen.

**Results:** Twenty-six lesions were suspected to be cancerous lesions by narrow-band imaging in the head and neck region. Sixteen lesions in 16 (35%, 16/46) patients were squamous cell carcinoma. Ten lesions were located in the hypopharynx and the remaining six lesions were located in the oropharynx. White light endoscopy could not point out any lesion.

**Conclusions:** Narrow-band imaging endoscopy can detect possible primary cancer in patients with primary unknown cervical lymph node metastasis.

*Key words: NBI – pharynx – primary unknown cancer – neck lymph node metastasis*

## INTRODUCTION

In the head and neck region, we sometimes treat patients with cervical lymph node metastasis where a primary tumor cannot be identified by laryngoscopy, computed tomography (CT) and magnetic resonance imaging (MRI). Primary unknown cervical lymph node metastasis (PUCLNM) is reported in 2–9% of metastases in the head and neck region. Additional work-up including upper gastrointestinal endoscopy can detect possible primary lesions in about 10% of the patients, but the possible primary site is not identified in 90% of the patients with PUCLNM.

The inability to find the primary tumor makes it difficult to decide on the most appropriate treatment for the patient, and the clinician must consider different options for the initial treatment. In some cases, the primary tumor is detected during treatment for the lymph node metastasis, but the primary site remains unidentified in some. In cases where the primary tumor is detected after the start of

treatment, it is impossible to switch the treatment. Thus, to stage and evaluate the treatment strategy, the clinician should be able to detect the primary site before starting treatment.

To find a primary lesion, blind biopsy (1–3) or tonsillectomy (4) is sometimes used in patients with PUCLNM. However, these surveillance methods do not always detect the primary lesion. In the case of PUCLNM, whole-neck irradiation will be indicated after cervical lymph node excision because we cannot pinpoint the primary cancer-based treatment strategy (5–7). Whole-neck irradiation causes adverse events such as salivary gland disorder, severe mucositis and taste disorder. In addition, if primary cancer could be detected after irradiation, re-irradiation would not be needed; this is important because surgery after irradiation increases the risk of leakage of the anastomosis.

Muto et al. (8,9) reported that narrow-band imaging (NBI) can detect superficial cancer in the oropharynx and hypopharynx. Although NBI is expected to help identify the primary lesion in patients with PUCLNM, there are no reports on this issue. We surveyed primary lesions in such patients using NBI endoscopy of the gastrointestinal tract.

## PATIENTS AND METHODS

From January 2003 to December 2006, 46 consecutive patients with PUCLNM were surveyed about the primary site using a gastrointestinal NBI endoscope in National Cancer Center Hospital East, Chiba, Japan. Written informed consent for the examination was obtained from all patients.

The definition of PUCLNM was in accordance with the report by Greenberg (10) as follows.

- It is proven to have malignant cells histologically.
- We cannot identify a primary tumor using ocular inspection or pharyngolarynx fiberoscopy.
- We cannot identify a primary tumor by CT or MRI.
- Other organs except the head and neck do not show a carcinoma.

In all patients, the possible primary tumor could not be detected by examination using CT, MRI, pharyngolaryngoscopy and standard white-light gastrointestinal endoscopy.

We used a magnifying videoendoscope (Q240Z, Olympus Medical Systems, Tokyo, Japan) and sequential RGB light source with NBI function (CLV-Q260SL, Olympus Medical Systems). The magnifying endoscope had a capability of $\times 80$ optical magnification. The NBI system has been described in detail in previous studies (8,9). In this system, the central wavelengths of NBI were 415 and 540 nm, and each had a bandwidth of 30 nm.

During the survey of the primary site in the head and neck region including the cervical esophagus, if the lesions showed both a well-demarcated brownish area and an irregular microvascular pattern (11), we diagnosed cancer. After this examination, we took a biopsy specimen to confirm the histological diagnosis.

## RESULTS

The patients' characteristics are shown in Table 1. Thirty-eight patients were men and eight were women. Their median age was 66 years (range, 38–81 years). Twenty-eight cases were N2 and 18 cases were N3. Thirty-one patients had metastatic lymph nodes in the upper jugular area (Level II), 13 had middle jugular lymph node metastasis (Level III) and 2 had lower jugular lymph node metastasis (Level IV).

Twenty-six lesions were suspected to be the cancerous site in 25 patients. Sixteen lesions in 16 patients were confirmed histologically as squamous cell carcinoma. Histological assessment of all of the possible primary lesions showed the similar feature of squamous cell carcinoma. Thus, primary cancer in the head and neck region was detected in 16 patients (35%) by NBI endoscopy. The patients' characteristics are shown in Table 2. Ten patients had metastatic lymph nodes in the upper jugular area, five had middle jugular lymph node metastasis and one had lower jugular lymph node metastasis. Nine cases were N3 and seven cases were N2. All of the lesions detected were superficial neoplasia. Ten lesions were located in the hypopharynx and the remaining six lesions were located in the oropharynx (three were tonsil). All lesions were T1 stage or Tis, and all lesions were $<2$ cm in size. Biopsy specimens revealed that one lesion was intraepithelial cancer and the other had invaded to the subepithelial layer.

**Table 1.** Patient characteristics

| | Patients |
|---|---|
| Age (years) | 66 (38–81) |
| Gender | |
| Male | 38 |
| Female | 8 |
| N stage | |
| N2a | 4 |
| N2b | 20 |
| N2c | 4 |
| N3 | 18 |
| Levels of cervical metastasis | |
| Upper jugular (II) | 31 |
| Middle jugular (III) | 13 |
| Lower jugular (IV) | 2 |

Thirty-eight patients were males and eight were females. Median age was 65 years (range, 38–81 years). Twenty-eight cases were N2 and 18 cases were N3. Thirty-one patients had metastatic lymph node in the upper jugular area (Level II), 15 had middle jugular lymph node metastasis (Level III) and 2 cases had lower jugular lymph node metastasis (Level IV).

**Table 2.** Characteristics of possible primary lesions detected by NBI

| | Primary | Endoscopic findings | *n* (levels) | Treatment |
|---|---|---|---|---|
| 1 | Oropharynx | Superficial | 3 (II) | CRT |
| 2 | Oropharynx | T1 | 3 (II) | CRT |
| 3 | Hypopharynx | Superficial | 3 (II) | RT |
| 4 | Oropharynx | Superficial | 3 (III) | CRT |
| 5 | Hypopharynx | Superficial | 3 (II) | CRT |
| 6 | Hypopharynx | Superficial | 3 (II) | EMR + ND |
| 7 | Hypopharynx | Superficial | 3 (II) | CRT |
| 8 | Hypopharynx | Superficial | 3 (II) | Surgery + ND |
| 9 | Oropharynx | Superficial | 2b (III) | Surgery + ND |
| 10 | Oropharynx | T1 | 2a (II) | Surgery + ND |
| 11 | Hypopharynx | Superficial | 2b (IV) | Surgery + ND |
| 12 | Hypopharynx | T1 | 2a (II) | Surgery + ND |
| 13 | Hypopharynx | Superficial | 2b (II) | EMR + ND |
| 14 | Hypopharynx | Superficial | 3 (III) | RT |
| 15 | Oropharynx | Superficial | 2c (II) | Surgery + ND |
| 16 | Hypopharynx | Superficial | 2b (III) | EMR + ND |

Nine cases were N3 and seven cases were N2. Five cases were treated by concurrent chemoradiation therapy and in nine cases, primary site was removed by surgery or endoscopic resection and they underwent neck dissection for lymph node metastasis. NBI, narrow-band imaging; CRT, chemoradiation therapy; EMR, endoscopic mucosal resection; ND, neck dissection.

**Figure 1.** Computed tomographic scan shows lymph node metastasis at left upper jugular area.

Five patients were treated by concurrent chemoradiation therapy (CRT). Two patients were treated with a chemotherapy regimen comprising 5-fluorouracil (800 mg/m$^2$, days 1–5) and cisplatin (80 mg/m$^2$, day 1). Two patients were treated with tegafur-gimeracil-oteracil potassium (60 mg/m$^2$, days 1–14) and cisplatin (20 mg/m$^2$, day 1). One patient was treated with cisplatin (80 mg/m$^2$, day 1). The irradiation field covered the whole neck, and the total radiation dose was 70 Gy (2 Gy/fr). Two patients were treated by radiation therapy (total 70 Gy) alone. For the other nine patients, the primary site was removed by surgery or endoscopic resection, followed by neck dissection of the lymph node metastasis. No patient received whole-neck irradiation after neck dissection.

Treatment of the 20 patients who cannot detect cancer lesion were CRT (for N3 or N2b), and neck dissection and close follow-up with NBI endoscopy (for N2a or N2b).

Figure 1 shows a representative case where the primary cancer was detected by NBI. This patient had a swollen lymph node (2.5 cm in size) on the left side of the upper jugular area (Level II) (Fig. 1). The specimen taken using a fine-needle aspiration method from the swollen lymph node revealed squamous cell carcinoma, which was confirmed later as metastatic. CT scan, MRI, laryngoscopy and standard gastrointestinal endoscopy could not detect any primary site. NBI detected easily a well-demarcated brownish area in the uvula to the right anterior palatine arch (Fig. 2B). In contrast, the conventional white-light image made it difficult to visualize the cancerous lesion (Fig. 2A). Magnifying the observation with NBI revealed easily an irregular microvascular pattern inside the lesion (Fig. 2D), but magnifying the observation with white light made it difficult to see this irregular microvascular pattern (Fig. 2C). We diagnosed cancer for this lesion. The biopsy specimen revealed squamous cell carcinoma, which was similar histologically to that of the metastatic lymph node. Treatment of this patient involved neck dissection and resection for primary disease, and we were able to avoid irradiation of the whole neck.

## DISCUSSION

We report for the first time that NBI endoscopy can detect possible primary cancer in patients with PUCLNM. Information about the primary site is very important for deciding on the appropriate treatment because the treatment strategy may differ for each primary site. Our data indicate that NBI can be helpful to the clinician when deciding on the treatment.

According to Greenberg (10), primary unknown carcinoma is defined when primary tumor cannot be detected by an autopsy. However, this definition cannot be applied in clinical decision-making. We defined a PUCLNM as one for which we could not detect any primary site by CT, MRI, laryngoscopy and gastrointestinal endoscopy (11). Although recent advance in technologies of CT, MRI and PET makes it possible to detect a small lesion precisely, the primary cancer is detected in only 2–9% of the patients with PUCLNM (1,2,12,13). Positron emission tomography (PET) or CT is also useful to detect occult cancer, but this primary site is too small to point out with PET. Random biopsy in the head and

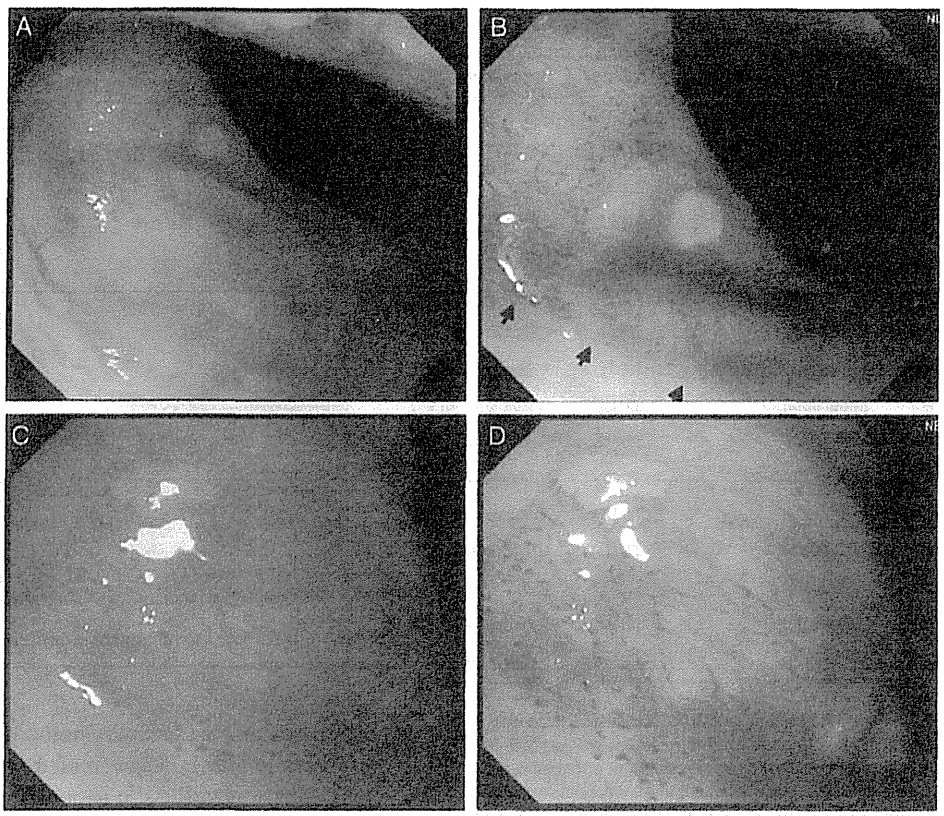


**Figure 2.** (A–D) Endoscopic findings. Conventional white-light image (A), narrow-band imaging (NBI) image (B), magnifying conventional white-light image (C) and magnifying the NBI images (D). NBI detected a well-demarcated brownish area in the uvula to right anterior palatine arch (B). In contrast, conventional white-light image was difficult to visualize the cancerous lesion (A). Magnifying the observation with NBI revealed an irregular microvascular pattern inside the lesion (D).

neck region may be useful for detecting possible primary cancer in patients with PUCLNM, but the detection rate is only around 10% (1,2). However, tonsillectomy is very useful to detect the primary cancer but tonsillectomy can detect only tonsil cancer. Because only 3 of 16 cases have a cancerous lesion on tonsil in this study, NBI endoscopy was better than tonsillectomy to detect occult tumor.

In the esophagus, Lugol chromoendoscopy is useful for detecting superficial squamous cell carcinoma. However, Lugol's solution cannot be applied in the head and neck region because of the risk of aspiration into the airway. NBI is now recognized as a useful and safe method for detecting superficial squamous cell carcinoma in the head and neck region because it uses no solution and improves the visibility. Muto et al. (8,9,16) reported that both a well-demarcated brownish area and an irregular microvascular pattern are typical characteristics of the superficial squamous cell carcinoma in the head and neck region. In this study, we evaluated the lesion according to these two endoscopic characteristics, and we were able to confirm 64% (16/25) of the lesions in the suspicious cancerous area as squamous cell carcinoma. This positive rate is better than that from a random biopsy (~10%). Finally, possible primary cancer could be detected in 35% (16/46) of the patients. These results indicate that NBI should be applied when surveying the primary site in patients with PUCLNM. Moreover, it is not impossible to detect cancerous lesion only using white-light endoscopy by trained endoscopist but NBI endoscopy is very easy for beginners to detect lesion.

Nine of 16 patients underwent surgery or endoscopic resection of the primary site and subsequent lymph node dissection. In such cases, post-operative whole-neck radiation is one treatment option (13–15). However, the indications for post-operative radiation therapy for PUCLNM are still controversial because these patients are at high risk for developing metachronous multiple cancers in the head and neck region (16). If they received radiation therapy as a post-operative radiation therapy, there is no radiotherapy treatment option for the later appearance of a metachronously developed second primary cancer in the head and neck region (14–16). The clinician must thus plan the post-operative radiation therapy carefully.

We cannot conclude with certainty whether the lesions detected by NBI were the true primary sites unless we identify their clonality. As a next step, we will compare the clonality of both primary sites and metastatic lymph nodes. In this study, at least, histological assessment showed the same histological features of the primary site and metastatic lymph

node. Clinically, histological accordance would be enough to consider whether the lesion is primary.

Although we could not evaluate the depth of invasion in all patients, we know that micro-invasive cancer can metastasize to the lymph node. The risk of lymph node metastasis of superficial squamous cell carcinoma is unknown, but collection of data from a large number of cases should help clarify this.

In conclusion, our data indicate that NBI has the potential to identify primary cancer in patients with PUCLNM. Identification of the primary site provides helpful information for deciding on the treatment strategy.

## Conflict of interest statement

None declared.

## References


1. Coker D, Casterline P, Chambers R, Jaques D. Metastases to lymph nodes of the head and neck from an unknown primary site. *Am J Surg* 1977;134:517–22.
2. Gluckman J, Robbins K, Fried M. Cervical metastatic squamous carcinoma of unknown or occult primary source. *Head Neck* 1990;12:440–3.
3. Jones A, Cook J, Phillips D, Roland N. Squamous carcinoma presenting as an enlarged cervical lymph node. *Cancer* 1993;72:1756–61.
4. Righi P, Sofferman R. Screening unilateral tonsillectomy in the unknown primary. *Laryngoscope* 1995;105:548–50.
5. Medini E, Medini A, Lee C, Gapany M, Levitt S. The management of metastatic squamous cell carcinoma in cervical lymph nodes from an unknown primary. *Am J Clin Oncol* 1998;21:121–5.
6. Jesse R, Perez C, Fletcher G. Cervical lymph node metastasis: unknown primary cancer. *Cancer* 1973;31:854–9.
7. McCunniff A, Raben M. Metastatic carcinoma of the neck from an unknown primary. *Int J Radiat Oncol Biol Phys* 1986;12:1849–52.
8. Muto M, Ugumori T, Sano YI, Otsu A, Yoshida S. Narrow-band imaging combined with magnified endoscopy for cancer at the head and neck region. *Dig Endosc* 2005;17:S23–4.
9. Muto M, Nakane M, Katada C, Sano Y, Ohtsu A, Esumi H, et al. Squamous cell carcinoma *in situ* at oropharyngeal and hypopharyngeal mucosal sites. *Cancer* 2004;101:1375–81.
10. Greenberg B. Cervical lymph node metastasis from unknown primary sites. An unresolved problem in management. *Cancer* 1966;19:1091–5.
11. Muto M, Katada C, Sano Y, Yoshida S. Narrow band imaging: a new diagnostic approach to visualize angiogenesis in superficial neoplasia. *Clin Gastroenterol Hepatol* 2005;3(7 Suppl 1):S16–20.
12. Nguyen C, Shenouda G, Black M, Vuong T, Donath D, Yassa M. Metastatic squamous cell carcinoma to cervical lymph nodes from unknown primary mucosal sites. *Head Neck* 16:58–63.
13. Mendenhall W, Million R, Cassisi N. Squamous cell carcinoma of the head and neck treated with radiation therapy: the role of neck dissection for clinically positive neck nodes. *Int J Radiat Oncol Biol Phys* 1986;12:733–40.
14. Freeman D, Mendenhall W, Parsons J, Million R. Unknown primary squamous cell carcinoma of the head and neck: is mucosal irradiation necessary? *Int J Radiat Oncol Biol Phys* 1992;23:889–90.
15. Coster J, Foote R, Olsen K, Jack S, Schaid D, DeSanto L. Cervical nodal metastasis of squamous cell carcinoma of unknown origin: indications for withholding radiation therapy. *Int J Radiat Oncol Biol Phys* 1992;23:743–9.
16. Muto M, Takahashi M, Ohtsu A, Ebihara S, Yoshida S, Esumi H. Risk of multiple squamous cell carcinomas both in the esophagus and the head and neck region. *Carcinogenesis* 2005;26:1008–12.

ELSEVIER

Auris Nasus Larynx 38 (2011) 271–275

AURIS NASUS LARYNX
INTERNATIONAL JOURNAL OF ORL & HNS

www.elsevier.com/locate/anl

# Window resection of the trachea and secondary reconstruction for invasion by differentiated thyroid carcinoma

Mitsuru Ebihara [a,*], Seiji Kishimoto [c], Ryuichi Hayashi [a], Masakazu Miyazaki [a], Takeshi Shinozaki [a], Hiroyuki Daiko [a], Masahisa Saikawa [a], Minoru Sakuraba [b], Shinpei Miyamoto [b]

[a] *Department of Head and Neck Surgery, National Cancer Center Hospital East, Japan*
[b] *Department of Plastic Surgery, National Cancer Center Hospital East, Japan*
[c] *Department of Head and Neck Surgery, Tokyo Medical and Dental University, Japan*

Received 3 February 2010; accepted 15 September 2010
Available online 18 November 2010

**Abstract**

*Objective:* In cases of differentiated thyroid carcinoma, the presence or absence of invasion into the circumferential organs is an important prognostic factor. Surgical procedures include circular resection of the trachea with end-to-end anastomosis and window resection with secondary closure. We have used window resection with secondary closure since 1993, and herein retrospectively analyze the treatment outcomes for this surgical procedure in order to determine the indications for procedure selection.
*Methods:* Subjects comprised 41 cases of invasion by differentiated thyroid carcinoma into the trachea, for which surgery was performed at the Department of Head and Neck Surgery of the National Cancer Center Hospital East from 1993 to 2007. The mean age was 65.7 ± 7.9 years, and the median length of the observation period was 43 months. There were 17 cases (41.4%) cases of secondary relapse.
*Results:* The 5-year and 10-year overall survival rates for this surgical procedure were 78.9% and 74.5%, respectively, while the 5-year and 10-year local control rates were 92.4% and 73.4%, respectively. The pathological resection stump was positive in 27 cases (65.8%), but no significant differences in treatment outcome were observed between the stump-positive group and the stump-negative group. There were 26 cases in which closure of the tracheal fistula was performed by the time of observation. When the tracheal defect had a diameter equivalent to 7 rings of the trachea or less and a circumference half that of the tracheal cartilage or smaller, including partial cricoid cartilage, it was possible to perform closure with only a local flap. For larger defects, reconstruction was performed using hard tissues or materials, such as hydroxyapatite, titanium mesh, and costal cartilage. There were 2 cases that required re-window because of dyspnea after closure.
*Conclusion:* The treatment outcomes for this surgical procedure for invasive cases of differentiated thyroid carcinoma into the trachea resulted in a low rate of local recurrence and similar survival rates as described in other reports. Even for cases of resection exceeding half the circumference of the trachea, closure of the tracheal fistula can be performed using hard tissues or materials; however, in such cases, we believe that closure should be attempted progressively in a two-stage reconstruction.


*Keywords:* Differentiated thyroid carcinoma; Tracheal invasion; Secondary reconstruction

## 1. Introduction

The prognostic factors for differentiated thyroid carcinoma include age, histopathological type, size of primary lesion, presence or absence of invasion into organs around the thyroid, and presence or absence of distant metastasis [1]. Treatment outcomes for differentiated thyroid carcinoma are generally good, but when invasion into the circumferential organs (trachea, larynx and cervical esophagus) occurs, it is necessary to resect those organs, thereby making treatment more difficult in many cases. The trachea and larynx are particularly susceptible to invasion,

* Corresponding author at: Department of Head and Neck Surgery, National Cancer Center Hospital East, Kashiwa-shi, Kashiwanoha 6-5-1, Chiba 277-8577, Japan. Fax: +81 04 7131 4724.
*E-mail address:* mebihara@east.ncc.go.jp (M. Ebihara).

0385-8146/$ – see front matter 
doi:10.1016/j.anl.2010.09.003

and this often causes problems for treatment. For cases of invasion into the trachea, circular resection, end-to-end anastomosis or window resection are mainly performed. We use a surgical procedure comprising resection of part of the trachea at the site of tumor invasion, temporary formation of a tracheal fistula, and secondary closure of the fistula. The advantage of this surgical procedure is that postoperative rest and fixation of the neck region are not necessary, and the airway can be secured with certainty. However, the resection margins are often close together or adjacent. Here, we examined the long-term treatment outcome of this surgical procedure and studied its validity and usefulness.

## 2. Patients and methods

Subjects comprised 41 cases diagnosed with invasion into the trachea before surgery and in which window resection of the trachea was performed, and these cases were selected from 338 cases of differentiated thyroid cancer for which surgery was performed at the Department of Head and Neck Surgery at the National Cancer Center Hospital East from 1993 to 2007, and we examined these cases retrospectively. On preoperative evaluation, subject cases included those in which invasion into the trachea was suspected based on CT and echo images and in which endoscopy detected redness or irregularity in the membrane of the tracheal lumen. The cases included 18 males and 23 females with a mean age of 65.7 ± 7.9 years, and the median observation period was 43 months (4–167 months). There were 24 cases undergoing initial treatment, including Stage IVA (22 cases) and Stage IV C (2 cases) cases, and there were 17 cases of secondary relapse, which comprised 41.4% of the total. And there were 22 cases with recurrent nerve paralysis before surgery.

## 3. Statistical analysis

Treatment outcomes were evaluated using the Kaplan–Meier method, and significant differences between the two groups were examined with the log-rank test.

## 4. Results

For all of the cases showing invasion into the trachea, window resection of the trachea (including cases of partial resection of the thyroid and cricoid cartilage) was performed, and there were no cases in which circular resection or end-to-end anastomosis were performed. In addition, there were 2 cases that required a free jejunal graft due to invasion into the esophagus. Although all cases were histopathologically diagnosed as papillary carcinoma, 4 of the cases presented with papillary carcinoma involving poorly differentiated components, and 1 case was papillary carcinoma involving anaplastic components. Histopathological evaluation of the resection stumps revealed that 27 of the 41 cases were stump positive (65.8%). In addition, no pathological findings of invasion into the trachea were observed in 2 cases. There were no cases in which radiation therapy was performed as an additional postoperative treatment.

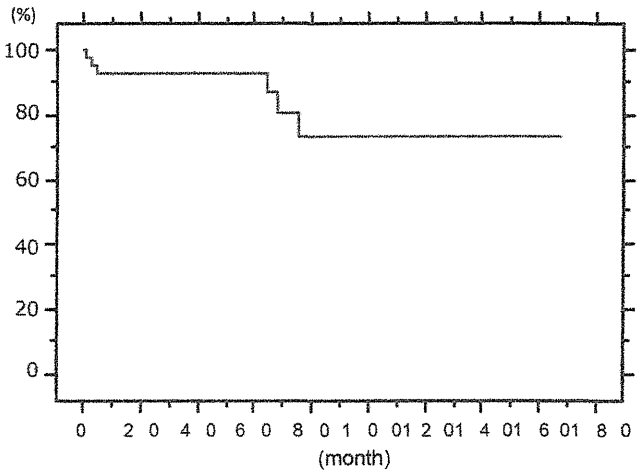


Fig. 1. Postoperative local control.

The 5-year and 10-year local control rates were 92.4% and 73.4%, respectively (Fig. 1), and the 5-year and 10-year overall survival rates were 78.9% and 74.5%, respectively (Fig. 2). For the pathological resection stumps, no significant differences were observed in the 5-year survival rates between the stump-positive and stump-negative groups (Fig. 3). Examination of the histopathological type in the 36 cases of papillary carcinoma and the 5 cases of papillary carcinoma involving poorly differentiated components and anaplastic components revealed that survival rates was significantly lower in the latter group ($p < 0.0001$). We included a case with poorly differentiated components on pathological findings, and death at 4 months after surgery was due to original disease by rapid regrowth in the neck and mediastinal lymph nodes. In addition, with regard to sex, age (older or younger than 65 years), the presence or absence of preoperative recurrent nerve paralysis, history of initial treatment or recurrence, and the presence or absence of

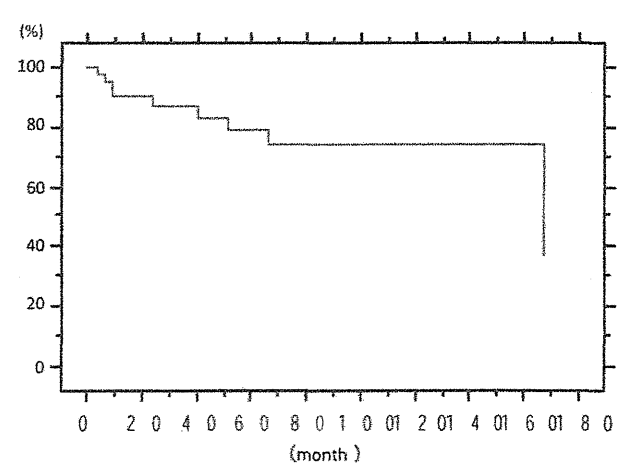


Fig. 2. Postoperative overall survival.

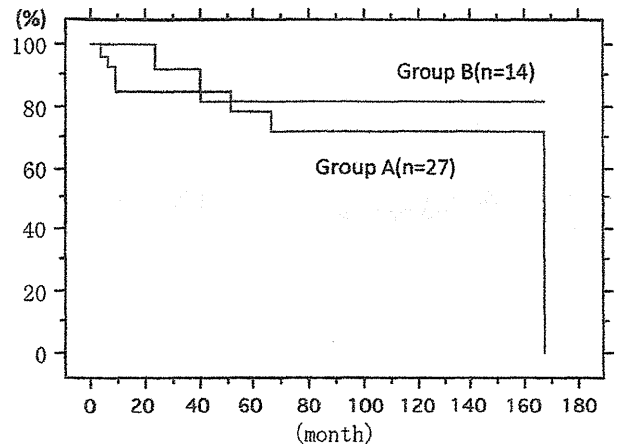


Fig. 3. Postoperative overall survival of group A (positive surgical stump) and group B (negative). No statistically significant differences were noted between the two groups ($p = 0.3359$).

lymph node relapse, no significant differences were observed in the treatment outcomes.

Prognoses were disease-free survival in 13 cases (31.7%), survival with cancer in 18 cases (43.9%), death due to the original disease in 9 cases (21.9%), and death due to other cancer in 1 case.

In the present study of local control, we observed 7 cases (17.1%) that appeared to recurrence from the resection stump. Among these 7 cases, 1 case was salvaged through total laryngectomy, while 4 cases resulted in death due to the original disease caused by rapid enlargement of the tumor, in which anaplastic conversion was suspected. There was only one case that required surgical management because of postoperative infection around the tracheal fistula. And there were 17 cases developed recurrent nerve paralysis after surgery.

Regarding the closure of the tracheal window area, complete closure was possible in 26 cases (63.4%) at the time of final observation. In 15 cases, we were unable to close the tracheal fistula, and there were 13 cases in which we did not attempt closure because of bilateral recurrent nerve paralysis or locoregional recurrence, and 2 cases that required re-windowing after closure.

The surgical procedure for closure involved the use of a local flap, such as a hinge flap, in 24 cases, and the range of the tracheal defects in these cases was, at maximum, equivalent to 7 rings of the trachea with a circumference of one-third to half. In cases for which complete closure was attempted using hard materials for defects with a wider range, complete closure was possible in 2 cases, while re-windowing was performed in 2 cases due to dyspnea after surgery. In the other cases, 2 cases ended in partial closure due to bilateral recurrent nerve paralysis. To determine the criteria for selection of the tracheal reconstruction operative method, the ranges for tracheal defect and reconstruction procedure, as well as the success and failure rates, are presented in Table 1. However, we excluded 13 patients who

Table 1
Range of resected areas for closure of tracheal fistula ($n = 28$).

| Tracheal rings | 1–4 | 5–7 | 8– |
|---|---|---|---|
| Circumference | | | |
| 1/3–1/2 | 18 | 6 | 1[a] |
| 1/2– | 2 (1[a]) | 1 | |

[a] Re-window for dyspnea after closure.

were not able to undergo closure of tracheal fistula as described earlier. In these cases, we attempted closure using a rotation flap or Deltopectoralis flap with hard tissues and materials such as thyroid cartilage, costal cartilage, titanium mesh and hydroxyapatite for defects more than half circumference or up to 10 rings of trachea. The 2 cases in which we used hydroxyapatite for such defects were closed progressively and perfect closure was possible.

## 5. Discussion

Organs that are susceptible to invasion in advanced cases of differentiated thyroid carcinoma include the trachea, the larynx and the esophagus. McCaffrey et al. noted that invasion into the trachea was observed in 37% of cases of local advanced papillary thyroid carcinoma, while invasion into the esophagus was observed in 21% of cases [2]. Typically, esophageal invasion remains limited to the muscle layer, and it is extremely rare for resection of all layers to be necessary. In fact, in the present study, all layers of the esophagus were resected and a free jejunal graft was required in only 2 cases.

For cases of invasion into the trachea, many reports have stated that if the invasion remains limited to the surface layer of the tracheal wall, it can be treated through a procedure known as shaving [3–5]. If the tumor can be completely resected through a macroscopic procedure, even if the tumor cells remain at the microscopic level, there is thought to be no effect on treatment outcome. However, when there is invasion reaching the lumen of the trachea, resection of all layers of the trachea is required. As the mode of invasion into the trachea, the Stage classifications proposed by Shin et al. have been widely used, and the cases in this study were mainly classified as Stage III or IV [6]. When a wide resection of the trachea is required in these cases, circular resection of the trachea and end-to-end anastomosis are often performed. The maximum range of tracheal resection that allows for simple end-to-end anastomosis is generally determined to be equivalent to 7 rings of the trachea or a major axis of 5–6 cm [3].

In addition, Shiba et al. reported that end-to-end anastomosis was possible for defects up to 7 cm. Furthermore, they needed to release the surrounding tissue for defects of 5 cm or more, and fixation of the neck region about 2 weeks after surgery [7]. Therefore, indications for surgery are limited in elderly patients if the range of tracheal resection becomes extensive. In circular resection, it is also

necessary to be aware of possible bilateral recurrent nerve paralysis, as in such cases, a postoperative tracheal fistula may be required. In particular, in some cases of recurrence, unilateral recurrent nerve paralysis has already been expressed, and it is necessary to be careful of bilateral recurrent nerve paralysis. Tracheostomy after end-to-end anastomosis should be avoided in most cases because of wound infection [8], while Shiba et al. suggested that it should be avoided in order to make a tracheal fistula around the anastomotic region.

We have avoided performing circular resection whenever possible for cases of invasion of differentiated thyroid carcinoma into the trachea that are Stage III or IV cases, in accordance with Shin et al., and we have instead employed a surgical procedure involving closure in two stages after window resection. In many cases of invasion of thyroid carcinoma into the trachea, lesions are unevenly distributed on either the left or right side, and it is believed that there are few cases that require circumferential resection. In addition, the greatest advantage of this surgical procedure is that the level of surgical invasiveness is lower than in cases of circular resection and the airway can be secured with certainty. The mean age of the cases in this study was relatively high, and there were many cases in which prognoses were not favorable. We believe that it is desirable to select a surgical procedure with as low a level of invasiveness as possible. In cases of window resection of the trachea, fixation of the neck region after surgery is not necessary. Regarding postoperative swallowing function, in a previously reported study of 30 cases, oral ingestion became possible after a mean period of 6 hospital days (1–55 hospital days) [9].

On the contrary, this procedure requires secondary closure of the tracheal fistula, and when the resection range is wide, hard tissues or materials are required to secure the lumen of the trachea during closure. According to a previous report, if the resection range of the trachea is small (i.e., in cases of resection with a range equivalent to 4 rings or less, and a circumference of half or less), closure can be performed using a local flap without any problems [9]. In addition, Suginoya et al. reported a case in which window resection of the trachea was performed because of invasion of thyroid carcinoma into the trachea [10]. In that case, auricular cartilage was used for secondary closure, but we have found no reports on limiting the surgical procedure and treatment outcomes for window resection over a wide range, or for closure of the fistula using hard tissues or materials.

In the present study, it was possible to perform closure using a local flap with a diameter equivalent to 7 rings of the trachea when the circumference of the defects ranged from one-third to half of that of the cartilage wall of the trachea, even in cases that included partial resection of the cricoid cartilage. Therefore, it is thought that partial resection of the cricoid cartilage unrelated to the success of closure. However, for defects with a circumference of over half, or with tracheal defects equivalent in diameter to up to 10 rings of the trachea, thyroidal cartilage, costal cartilage, titanium mesh or hydroxyapatite are used, and a rotation flap or Deltopectoralis flap is used to perform closure. In 2 cases in which hydroxyapatite was used for defects with a circumference of over half, complete closure was possible using a 2-stage gradual procedure. In addition, in both of the cases in which dyspnea occurred after closure and re-windowing was performed, closure was attempted in a single procedure after the initial surgery (Figs. 4–6). Based on these findings, in cases of defects with a wide range requiring the use of hard tissues or materials, we suggest partial closure after waiting for scar formation around the fistula, after which gradual closure is safer. Moreover, in cases of wide invasion in the direction of the major axis (10 rings of the trachea was the longest in the present study), end-to-end anastomosis should be selected based on tumor invasion, but this surgical procedure can be applied due to its low invasiveness. About hard materials, we found that hydroxyapatite is useful, but we cannot use it for surgery because this material is unauthorized by Pharmaceutical Affairs Act in Japan at present. So we prefer to use costal cartilage because of moderate rigidity or titanium mesh for wide defect.

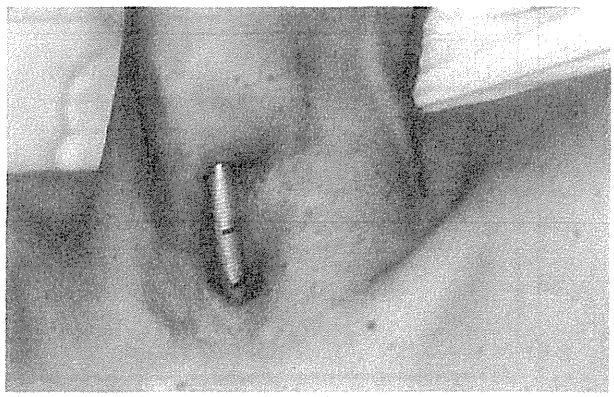

Fig. 4. Tracheal defects (3 rings including partial cricoid resection, and more than half of tracheal circumference).

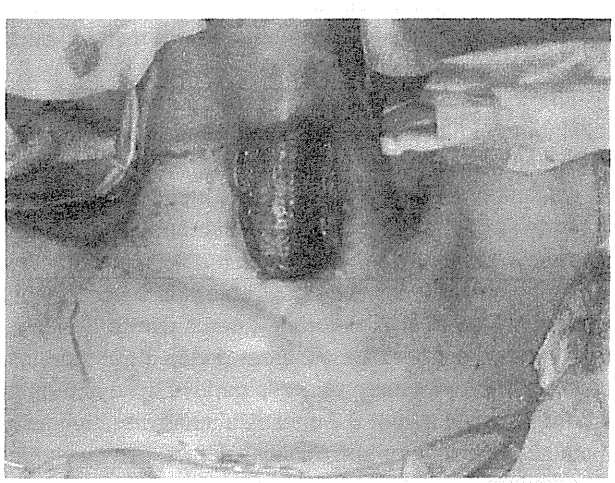

Fig. 5. Secondary closure using titanium mesh.

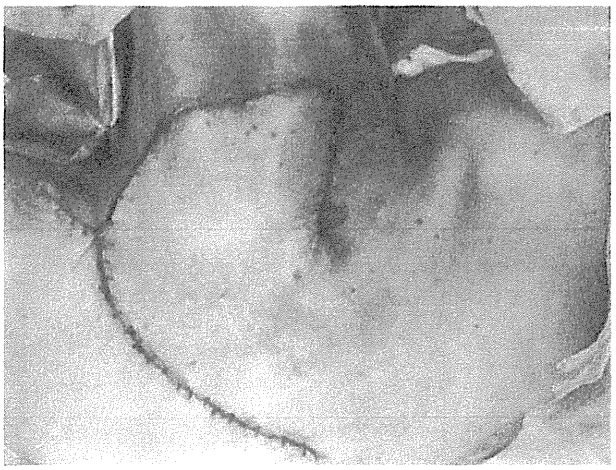

Fig. 6. Closure with rotation flap. However, re-windowing was required because of dyspnea.

With regard to treatment outcomes, there have been many reports that the 5-year survival rate in cases of thyroid carcinoma with invasion into the aerodigestive system is approximately 60–80%. Nishida et al. reported that the 5-year survival and local recurrence rates of circular resection in cases of invasion into the deep layers of the trachea were 67% and 7.5%, respectively [11]. McCaffrey et al. reported that the 5-year and 10-year survival rates were 79% and 63%, respectively [2], and Andersen et al. reported that the 5-year and 10-year survival rates were 60% and 50%, respectively [12]. The present study found similar outcomes as these other reports using circular resection, and in cases of differentiated thyroid carcinoma in which the treatment outcome is believed to be relatively favorable, the long-term prognosis for surgery in cases of invasion into the circumferential organs, particularly the trachea, is not always favorable. We need longer follow-up periods in future studies because of the slowly growing tumor. However, in the present study, local recurrence was often rapid, usually due to anaplastic transformation with regional metastasis or distant metastasis during the postoperative follow-up period. With regard to the reasons for complete closure of the fistula in approximately 60% of cases, this was largely due to bilateral recurrent nerve paralysis and the disease course.

In this histopathological comparative study of resection stumps, no significant differences were observed between the survival rates for cases in which the resection stump was positive and cases in which the resection stump was negative. In addition, the local stump recurrence rate was relatively low, and it is therefore believed that even in cases of invasion of differentiated thyroid carcinoma into all layers of the trachea, if complete resection can be performed through a macroscopic procedure, the necessity of complete pathological resection is reduced.

Considering the prognosis of tracheal invasion cases, we believe that the present surgical procedure is valid and appropriate due to its low invasiveness. For extensive tracheal defects, it is hoped that tracheal regenerative therapy will be possible in the future [13].

## 6. Conclusions

There were no significant differences between the treatment outcomes for cases of complete pathological resection and cases of incomplete resection, and local control was highly favorable, indicating that the implementation of window resection of the trachea and secondary closure is an appropriate surgical procedure for cases of invasion of differentiated thyroid carcinoma into the trachea. In addition, due to its low invasiveness, this procedure can be used safely in elderly patients. This surgical procedure is particularly useful for cases in which the range of invasion is limited to half the circumference of the tracheal wall or less, and for cases with wider defects, it is also possible to safely perform closure of the tracheal fistula by conducting reconstructive procedures in two stages using hard tissues or materials.

## References

[1] Shah JP, Loree TR, Dharker D, Strong EW, Begg C, Vlamis V. Prognostic factors in differentiated carcinoma of the thyroid gland. Am J Surg 1992;164:658–61.
[2] McCaffrey TV, Bergstralh EJ, Hay ID. Locally invasive papillary thyroid carcinoma: 1940–1990. Head Neck 1994;16:165–72.
[3] Czaja JM, McCaffrey TV. The surgical management of laryngotracheal invasion by well-differentiated papillary thyroid carcinoma. Arch Otolaryngol Head Neck Surg 1997;123:484–90.
[4] Kowalski LP, Filho JG. Result of the treatment of locally invasive thyroid carcinoma. Head Neck 2002;24:340–4.
[5] Gillenwater AM, Goepfert H. Surgical management of laryngotracheal and esophageal involvement by locally advanced thyroid cancer. Semin Surg Oncol 1999;16:19–29.
[6] Shin DH, Mark EJ, Suen HC, Grillo HC. Pathologic staging of papillary carcinoma of the thyroid with airway invasion based on the anatomic manner of extension to the trachea: a clinicopathologic study based on 22 patients who underwent thyroidectomy and airway resection. Hum Pathol 1993;24:866–970.
[7] Shiba K, Nagata H, Numata T. Primary reconstruction of airway by end-to-end anastomosis after resection of the upper trachea and cricoids cartilage. Jpn Bronchoesophagol Soc 2008;59:414–21.
[8] Price DL, Wong RJ, Randolph GW. Invasive thyroid cancer: management of the trachea and esophagus. Otolaryngol Clin N Am 2008;41:1155–68.
[9] Ebihara M, Ebihara S, Kishimoto S, Saikawa M, Hayashi R, Onitsuka T, et al. Surgical treatment of differentiated thyroid cancer with tracheal invasion. J Otolaryngol Jpn 1998;101:1406–11.
[10] Sugenoya A, Matsuo K, Asanuma K, Shingu T, Masuda H, Kobayashi S, et al. Management of tracheal wall resection for thyroid carcinoma by tracheocutaneous fenestration and delayed closure using auricular cartilage. Head Neck 1995;17:339–42.
[11] Nishida T, Nakao K, Hamaji M. Differentiated thyroid carcinoma with airway invasion: indication for tracheal resection based on the extent of cancer invasion. J Thorac Cardiovasc Surg 1997;114:84–92.
[12] Andersen PE, Kinsella J, Loree TR, Shaha AR, Shah JP. Differentiated carcinoma of the thyroid with extrathyroidal extension. Am J Surg 1995;170:467–70.
[13] Omori K, Tada Y, Suzuki K, Nomoto Y, Matsuzuka T, Kobayashi K, et al. Clinical application of in situ tissue engineering using a scaffolding technique for reconstruction of the larynx and trachea. Ann Otol Rhinol Laryngol 2008;117:673–8.

Cancer Science
The official journal of the Japanese Cancer Association JCA

# Phase I trial of chemoradiotherapy with the combination of S-1 plus cisplatin for patients with unresectable locally advanced squamous cell carcinoma of the head and neck

Makoto Tahara,[1,4,5] Hironobu Minami,[2,6] Mitsuhiko Kawashima,[3] Kenji Kawada,[2,7] Hirofumi Mukai,[2] Minoru Sakuraba,[4] Kazuto Matsuura,[4,8] Takashi Ogino,[3] Ryuichi Hayashi[4] and Atsushi Ohtsu[1]

[1]Departments of Gastroenterology and Gastrointestinal Oncology, [2]Hematology and Medical Oncology, [3]Radiation Oncology, and [4]Head and Neck Oncology & Plastic and Reconstructive Surgery, National Cancer Center Hospital East, Chiba, Japan

(Received July 2, 2010/Revised November 5, 2010/Accepted November 10, 2010/Accepted manuscript online November 15, 2010/Article first published online December 7, 2010)

**The aim of the present study was to determine the maximum tolerated dose (MTD) of S-1 in combination with chemoradiotherapy (CRT) in patients with unresectable locally advanced squamous cell carcinoma of the head and neck, and evaluate the difference in pharmacokinetics of S-1 when administered as a suspension via a feeding tube or orally as a capsule. Chemotherapy consisted of administration of S-1 twice daily on days 1–14 at escalating doses of 40, 60 and 80 mg/m$^2$ per day, and cisplatin at 20 mg/m$^2$ per day on days 8–11, repeated twice at a 5-week interval. Single daily radiation of 70 Gy in 35 fractions was given concurrently starting on day 1. Two additional cycles of chemotherapy were planned after the completion of CRT. Before starting CRT, each patient received S-1 via two different administration methods. Twenty-two patients were enrolled. The MTD was reached with S-1 at 80 mg/m$^2$ per day, with two of six patients experiencing febrile neutropenia lasting more than 4 days. All four patients whose creatinine clearance was decreased to <60 mL/min after the first cycle of chemotherapy developed febrile neutropenia lasting more than 4 days. Pharmacokinetic analysis revealed that the 5-fluorouracil area under the curve did not significantly differ by the administration route. S-1 at 60 mg/m$^2$ per day for 14 days was well tolerated with concurrent CRT. Administration of S-1 as a suspension or by whole capsule can be considered therapeutically interchangeable. Although these data are preliminary, activity was highly promising, and this approach warrants further investigation. (*Cancer Sci* 2011; 102: 419–424)**

Head and necks cancers are the sixth most common cancer in the world, and approximately 500 000 new cases are projected annually.[1] An estimated 60% of these patients will present with locally advanced disease (stage III/IV).

In the last 20 years, the integration of concurrent chemoradiotherapy (CRT) has advanced the treatment of locoregionally advanced squamous cell carcinoma of the head and neck (SCCHN), improving locoregional control and overall survival (OS) compared with radiotherapy (RT) alone while allowing organ preservation. However, half of these cases will recur, indicating a clear need for further therapeutic intervention. Moreover, although ample data provide a high level of evidence for the benefit of platinum-based CRT for unresectable locally advanced SCCHN,[2] an optimal CRT regimen is yet to be defined.

S-1 is a novel oral fluoropyrimidine derivative that consists of tegafur, 5-chloro-2, 4-dihydroxypyridine (CDHP) and potassium oxonate (Oxo) at a molar ratio of 1:0.4:1. Tegafur is a prodrug of 5-fluorouracil (5-FU).[3] CDHP augments the activity of 5-FU by inhibiting dihydropyrimidine dehydrogenase (DPD). Oxo reduces gastrointestinal (GI) toxicity by inhibiting orotate phosphoribosyl transferase and 5-FU phosphorylation in intestinal mucosa.

S-1 has been shown to be active against head and neck cancer, producing a response rate of 34%.[4] The combination of cisplatin (CDDP) and S-1 shows promising activity (response rate 67.6%) with acceptable toxicity for locally advanced head and neck cancer.[5] The combination of S-1 and fractionated radiotherapy is more effective against human oral cancer xenografts than either modality alone.[6]

A previous study demonstrated that the combination of S-1 and fractionated radiotherapy was more effective against human oral cancer xenografts than either treatment alone,[6] while another demonstrated that S-1 had a greater effect on radiosensitivity in human non-small-cell lung cancer xenografts in mice than uracil/tegafur (UFT), which also is an oral fluoropyrimidine derivative but does not contain CDHP.[7,8] CDHP enhanced radiosensitivity in human lung cancer cells in a dose escalation-dependent manner, suggesting that S-1 might be a more powerful enhancer of radiosensitivity in cancer than 5-FU or UFT.

Against this, however, no study has reported the feasibility and safety of S-1 in combination with CRT in patients with locally advanced SCCHN. We therefore conducted a single institutional, phase I, dose-escalation study of S-1 in combination with CRT in patients with unresectable locally advanced SCCHN.

Because CRT not only improves locoregional control but also exacerbates toxicities such as mucositis and dysphagia, patients may have difficulty in swallowing capsules. S-1 should therefore be administered as a suspension via a feeding tube. To date, however, no adequate bioavailability data for S-1 when administered as a suspension via a feeding tube has been available. For this reason, we also evaluated the difference in pharmacokinetics of S-1 when administered as a suspension via a feeding tube or orally by capsule.

## Patients and Methods

**Eligibility.** Eligibility for the present study required a histologically or cytologically confirmed diagnosis of SCCHN with unresectable locally advanced disease, including postoperative local recurrence. Careful evaluation for unresectability was required from a multidisciplinary conference, which included head and neck surgeons, radiation oncologists and medical

[5]To whom correspondence should be addressed. E-mail: matahara@east.ncc.go.jp
Present addresses:
[6]Medical Oncology, Kobe University Graduate School of Medicine, Kobe, Japan.
[7]Medical Oncology, Japanese Red Cross Nagoya Daiichi Hospital, Nagoya, Japan.
[8]Department of Head and Neck Surgery, Miyagi Cancer Center, Natori, Japan.

doi: 10.1111/j.1349-7006.2010.01799.x

oncologists. Criteria for unresectability were carefully defined as follows: (i) technical unresectability, considered to mean tumors fixed to the carotid artery, mastoid, base of the skull or cervical spine; and (ii) physician determination of low surgical curability based on neck lymph node metastases such as N2c-3. Medical unsuitability for resection was not sufficient for patient eligibility; eligibility also required an Eastern Cooperative Oncology Group (ECOG) performance status of 0 or 1, age 20–75 years and adequate organ function. Written informed consent was required from all patients before the start of any therapy.

Patients were excluded if they had any of the following conditions: previous chemotherapy or radiotherapy; concurrent active malignancy except excised intramucosal gastric or esophageal cancer that could be removed by endoscopic mucosal resection; pharyngeal fistula; active bleeding from the GI tract; active infection; serious medical problem that might interfere with the achievement of study objectives; pregnancy or lactation; or expected survival <3 months.

**Treatment.** Baseline evaluation included patient history, physical examination, panendoscopy, dental evaluation, head and neck magnetic resonance imaging (MRI), computed tomography (CT) scan of the chest and abdomen, routine laboratory studies and electrocardiography (EKG). The treatment schedule is shown in Fig. 1.

Radiotherapy was done with 70 Gy/35 fractions over 7 weeks using six mega volt (MV) X-ray and 3-D radiotherapy techniques, and was started on day 1. Intensity-modulated radiotherapy was unavailable during this study. Gross tumor volume (GTV) was determined based on endoscopic or radiographic findings. Clinical target volume (CTV) was defined by adding 0.5 to 1 cm to the GTV. Planning target volume (PTV) was determined by adding appropriate margins to the CTV with consideration for physiological organ motion and daily set-up error. All patients underwent prophylactic nodal irradiations encompassing bilateral upper, middle and lower jugular, accessory and retropharyngeal lymph nodes up to 40–46 Gy. An additional 24–30 Gy was added to the PTV. Maximum dose to the spinal cord was restricted to 46 Gy, and posterior neck node was boosted using a 9–12 MeV electron beam as indicated. The radiotherapy dose was prescribed to the midplane along the beam axis, and dose deviation within the PTV was restricted to ±5% of the prescribed dose.

Chemotherapy consisted of administration of S-1 twice daily on days 1–14 at escalating doses of 40, 60 and 80 mg/m$^2$ per day, and 2-h infusion of CDDP at 20 mg/m$^2$ per day on days 8–11, repeated twice with a 5-week interval. Hydration consisted of 1 L of normal saline solution over 2 h prior to CDDP, as well as mannitol 12.5 gm by i.v. bolus infusion and 2 L of normal saline solution over 4 h following CDDP administration. Two additional cycles of S-1 and CDDP at the same dose level of CRT, repeated with a 4-week interval, were planned 4 weeks after the completion of CRT. Neutrocytes had to have recovered to at least 2000 cells/mm$^3$ and grade 1 creatinine or >50 mL/min of creatinine clearance was required by the time of the next cycle.

All patients underwent emplacement of a percutaneous endoscopic gastrostomy (PEG) feeding tube prior to the initiation of treatment. Prophylactic use of granulocyte-colony stimulating factor was not permitted. Additional treatment was not permitted unless persistent disease or disease progression was observed. When a patient had persistent or recurrent disease at the completion of CRT, surgical salvage was considered.

**Toxicity.** Toxicities were evaluated according to the National Cancer Institute Common Toxicity Criteria for Adverse Events (NCI-CTCAE) version 2.0. Any of the following adverse events observed within 30 days after the completion of CRT was deemed a dose-limiting toxicity (DLT): (i) febrile neutropenia lasting more than 4 days; (ii) grade 4 thrombocytopenia; (iii) grade 3 or 4 non-hematological toxicities except grade 3 anorexia, nausea, vomiting, stomatitis, esophagitis, infection due to stomatitis, dysphagia and skin toxicity; (iv) cessation of treatment due to an adverse event; or (v) treatment-related death. The maximum-tolerated dose (MTD) was defined as the dose at which more than two of six patients experienced a DLT. The recommended safe dose for further study was assessed at the dose level immediately below the MTD.

A minimum of three assessable patients was treated at each dose level. If one of the three patients at a given dose experienced a DLT, three more patients were accrued at the same dose level. If more than two of six patients at a given dose experienced a DLT, three more patients were treated at the next lower dose level. If less than one of six patients experienced a DLT, an additional six patients were accrued at the same dose level to determine the recommended dose.

**Sample collection.** Before the initiation of CRT, patients who gave consent underwent pharmacokinetic investigation. A single dose of S-1 as a capsule formulation was administrated orally 4 days before the start of CRT (day -4), while the same dose was given through a feeding tube as a suspension 2 days before the start of CRT (day -2). Suspensions were prepared by simple dissolution of a S-1 capsule in hot water. Peripheral blood samples were drawn before and at 0.5, 1, 2, 4, 6, 8, 10 and 24 h after each administration. Heparinized blood was centrifuged at 3000 rpm for 15 min at 4°C, and plasma was stored at −80°C.

**Pharmacokinetic analysis.** Tegafur, 5-FU, CDHP and Oxo were analyzed according to the method of Matsushima *et al.*[9] Pharmacokinetic parameters of Tegafur, 5-FU, CDHP and Oxo were estimated according to a standard noncompartmental method. Maximum plasma concentration ($C_{max}$) and time to $C_{max}$ ($T_{max}$) were taken from the observed data. The area under the plasma-concentration time curve (AUC) for time 0 to infinity was estimated by summing AUC from 0 to time t ($AUC_{0-t}$) and $C_{tlast}/k$, where $C_{tlast}$ was the concentration at the last measured point. The apparent rate constant of elimination ($k$) was estimated by linear regression on the logarithm of the plasma

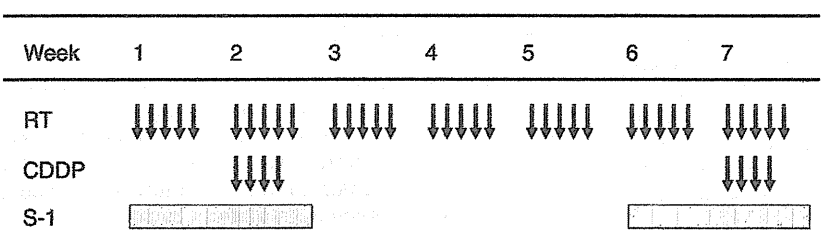


RT: 2 Gy/Fr x 33 or 35 Fr (total 70 Gy)
CDDP: 20 mg/m$^2$/day, iv, days 8–11, days 43–46
S-1: 40, 60, 80 mg/m$^2$/day, twice daily po, days 1–14, days 36–49

**Fig. 1.** Treatment schedule. Two additional cycles of S-1 and cisplatin (CDDP) at the same dose level of the chemoradiotherapy (CRT), repeated at a 4-week interval, were planned 4 weeks after the completion of the CRT. RT, radiotherapy.



doi: 10.1111/j.1349-7006.2010.01799.x

concentrations versus time, and $AUC_{0-t}$ was estimated using the log trapezoidal method.

**Criteria for response.** Tumor responses were evaluated according to Response Evaluation Criteria in Solid Tumors (RECIST) by panendoscopy, MRI of the head and neck and CT scan of the chest and abdomen.

**End-points and statistical methods.** The primary end-point in the present study was the MTD and DLT of S-1 in combination with a fixed dose of CDDP and RT. Safety and feasibility of this treatment were evaluated in patients with unresectable locally advanced SCCHN. Secondary end-points included complete response rate, progression-free survival (PFS), locoregional PFS, overall survival (OS) and pharmacokinetics of S-1 when administered as a suspension via the feeding tube.

The survival curve was estimated using the Kaplan–Meier method. Safety and efficacy analyses were both conducted on an intention-to-treat (ITT) population, defined as all patients enrolled in the study who received at least one dose of RT. A subject's PFS was defined as the time from the date of the first administration of CRT to the first documentation of disease progression, subsequent therapy or death. The OS was determined from the date of the first administration of CRT to the date of death or the last confirmed date of survival. Locoregional PFS was defined as the time from the date of the first administration of CRT to the first documentation of locoregional disease progression. Statistical data were obtained using the SPSS software package (SPSS 11.0 Inc., Chicago, IL, USA).

This study was conducted at the National Cancer Center Hospital East. The protocol was approved by the Institutional Review Board at the National Cancer Center.

## Results

**Patient and disease characteristics.** Twenty-two patients were enrolled between February 2003 and January 2005. One patient did not receive CRT because it made the performance status worse due to disease progression, leaving 21 patients in the ITT population. Patient characteristics in the ITT population are listed in Table 1. The most common site of the primary lesion was the hypopharynx (59%). One patient had unresectable local recurrence after total larnyngectomy for hypopharyngeal cancer and the other 20 had never received any prior treatment for head and neck cancer.

**Treatment administration.** A total of 69 cycles of chemotherapy was administered. The number of cycles was two in seven patients, three in three patients, four in 10 patients and six in one patient. The reasons for the administration of less than four cycles were toxicities ($n = 2$), physician decision due to concern about tolerance ($n = 2$) and patient refusal due to achievement of complete remission ($n = 6$). One patient received six cycles due to persistent disease that could not be removed by salvage surgery.

Three patients were treated at the dose level of S-1 40 mg/m$^2$ without DLT. Of the first three patients who received S-1 at the 60 mg/m$^2$ dose level, one patient blacked out after straining at stool due to constipation on day 16 and developed grade 3 ischemic colitis, but reported recovery within 1 week under conservative treatment including hydration. Because he finished taking S-1 on day 14 and did not develop any GI toxicity including mucositis or diarrhea before suffering from this colitis, the safety committee decided that this colitis was not likely related to the study treatment. Two other patients had no DLT and dose escalation subsequently proceeded. Of the first three patients treated at a dose level of S-1 80 mg/m$^2$, one developed febrile neutropenia lasting more than 4 days, leading to the accrual of an additional three patients at this level. Thus, six patients were treated at the dose level of S-1 80 mg/m$^2$, of whom two developed febrile neutropenia lasting more than 4 days. The MTD was therefore set at 80 mg/m$^2$ per day of S-1.

**Table 1. Patients' characteristics**

| Characteristic | No. patients ($n = 21$) |
|---|---|
| *Age (years)* | |
| Median | 62 |
| Range | 45–73 |
| *Sex* | |
| Male | 19 |
| Female | 2 |
| *ECOG performance score* | |
| 0 | 15 |
| 1 | 6 |
| *Site of primary tumor* | |
| Hypopharynx | 13 |
| Pharynx | 1 |
| Oropharynx | 5 |
| Nasopharynx | 2 |
| *AJCC stage* | |
| IV | 20 |
| Local relapse | 1 |
| *T stage* | |
| T1 | 4 |
| T2 | 5 |
| T3 | 3 |
| T4 | 8 |
| Local relapse | 1 |
| *N stage* | |
| N0 | 3 |
| N2a | 1 |
| N2b | 2 |
| N2c | 6 |
| N3 | 8 |

AJCC, American Joint Committee on Cancer.

Three additional patients were treated at the dose level of S-1 60 mg/m$^2$, one of whom experienced grade 3 diarrhea with grade 3 infection. To determine the recommended dose of S-1, six additional patients (total of 12 patients) were treated at the dose level of S-1 60 mg/m$^2$, three of whom developed febrile neutropenia lasting for more than 4 days. One of them experienced febrile neutropenia lasting for 2 weeks despite using granulocyte colony-stimulating factor supports and the diagnosis of myelodysplastic syndrome was made by bone marrow study. One week after the completion of CRT, another of these three patients who experienced febrile neutropenia developed grade 3 diarrhea, which occurred 1 day after the development of febrile neutropenia. Because the administration of S-1 had finished 1 week previously, this diarrhea was not related to S-1 but to the neutropenia or antibiotic drugs, and was not regarded as a DLT.

During CRT, eight patients (38%) received administration of S-1 via a feeding tube, and a total of 14% of the planned doses of S-1 were administered via a feeding tube during CRT. The number of patients who received S-1 via a feeding tube at each dose level was one of three at 40 mg/m$^2$, four of 12 at 60 mg/m$^2$ and three of six at 80 mg/m$^2$.

All patients were treated with conventional 3-D RT and received planned doses of CDDP. One patient received a total of 68 Gy while the other 20 received 70 Gy. Four patients required the splitting of RT due to adverse events, including colitis in one patient, grade 3 dermatitis and infection in one patient and neutropenia in two patients. Of the two patients who developed neutropenia, one was treated at the dose level of S-1 80 mg/m$^2$, while the second was treated at 60 mg/m$^2$.

**Toxicity.** Overall toxicities during treatment are listed in Table 2. Grade 3 or 4 toxicities by the S-1 dose level are listed in Table 3. The incidence of grade 3 or 4 neutropenia and febrile neutropenia increased with increasing dose, with half of those